Host-parasite interactions of an avian blood parasite elucidated by single-cell transcriptomics

Tim Maximilian Rapp[1], Tobias Lautwein[2], Robert Peuß[3,4], Joachim Kurtz[4,5], Oliver Krüger[1,5], Nayden Chakarov[1,5]

[1]Department of Animal Behaviour, Bielefeld University, Germany

[2]Biologisch-Medizinisches Forschungszentrum (BMFZ), Heinrich-Heine-Universität Düsseldorf, Germany

[3]Institute for Integrative Cell Biology and Physiology, University of Münster, Germany

[4]Institute for Evolution and Biodiversity, University of Münster, Germany

[5]JICE, Joint Institute for Individualisation in a Changing Environment, University of Münster and Bielefeld University, Germany

Correspondence:

Tim Maximilian Rapp

Department of Animal Behaviour

Bielefeld University

Konsequenz 45

33615 Bielefeld

E-mail: timrapp@hotmail.de

Abstract

To date, the intricate cellular and molecular interplay between hosts and parasites is well described for only a limited number of model systems. Recent methodological advances now allow deep insights into non-model host-parasite interactions, including intense reciprocal manipulations. We applied single cell RNA-sequencing to blood samples of wild, long-lived avian hosts, infected with the malaria-like parasite *Leucocytozoon*. We identified host cell types and the molecular toolkits involved in host immunity and parasite virulence. Comparing blood cell-type specific transcriptomic profiles between hosts with low and high parasitaemia indicates tools of parasitic immune evasion and potential modulation of the host immune response. In line with the reportedly low pathogenicity of the parasite, the response of immune cells was overall low. This lack of antagonism likely represents a result of long-lasting coevolution. Our study illuminates in rare detail a rather benign non-model host-parasite interaction and bridges the large phylogenetic gap along the evolutionary gradient from parasitism to mutualism. The cell-type specific markers identified will be useful in advancing our understanding of the evolutionary forces shaping host immunity.

Key words: Host-parasite interaction, avian malaria, scRNA-seq, transcriptomics, immunosuppression, host response, *Leucocytozoon*, *Plasmodium*

27 Parasites represent a significant proportion of biodiversity and have evolved to manipulate host
28 defences in diverse ways[1–3]. On an evolutionary scale, this variability of fitness effects ranges from
29 mutualism to parasitism and may be maintained by a trade-off between transmission and virulence[4–
30 9]. Conversely, host immune responses cause costs to parasites which vary strongly among and within
31 species[10]. For example, possible courses of human malaria range from clearance, over asymptomatic
32 and uncomplicated forms, to severe malaria and death[11].

33 The complex lifecycles of intracellular protozoans involve many mechanisms for the invasion of host
34 cells and evasion of the immune system[12–15]. In well-characterised malaria parasites of the genus
35 *Plasmodium*, some of these mechanisms include antigenic variation, dysregulation of B cells, anergy
36 of T-cells and concomitant immunosuppression[13,14].

37 Despite their long-established role as models of evolutionary ecology, many aspects of the biology of
38 avian malaria and malaria-like parasites remain enigmatic[16]. Here, we focus on *Leucocytozoon*, which
39 is phylogenetically distant from its haemosporidian sister genera *Plasmodium* and *Haemoproteus*[17]. A
40 comparatively high host specificity of *Leucocytozoon* occurs, with far more than a hundred different
41 *Leucocytozoon* species, each specialised on a small range of bird species[18]. Especially in birds of prey a
42 number of specialist parasite lineages occur, suggesting a long history of co-adaptation between
43 *Leucocytozoon* and their hosts[19].

44 Unlike other haemosporidians, *Leucocytozoon* is capable of infecting diverse hosts cell types, including
45 different leukocytes[18]. Furthermore, some *Leucocytozoon* species achieve high prevalence and
46 infection intensity, while displaying apparently low virulence[20–23]. In an intensively-studied population
47 of Common Buzzards in Germany *L. toddi*-infections occur at a prevalence of up to 86% (unpublished
48 data). With its distinct infection biology, high prevalence and evolutionary trajectory, this taxon allows
49 us to annotate a case of rather mutualistic co-adaptation within the wide range of host-parasite
50 interactions.

51 The *Leucocytozoon* lifecycle includes merozoite stages invading erythroblasts, erythrocytes and
52 mononuclear leukocytes within the host. Macro- and microgametocytes ("female" and "male"-type
53 precursors, respectively) then develop in the infected cells. Gametogenesis is initiated upon ingestion
54 by blackflies (Simuliidae)[18]. The remarkable morphological or physiological changes performed by
55 these parasites and the cells harbouring them throughout their lifecycle have so far never been linked
56 to context-dependent transcriptional changes.

57 Very few studies have investigated the transcriptomic responses to haemosporidian infections in wild
58 birds and those have so far only analysed whole blood transcriptomes, potentially convoluting cell-
59 type specific expression changes[24–27]. Meanwhile single cell RNA-sequencing (scRNA-seq) has become
60 capable of filling this potential gap, with first advances in mapping immune cells in two domestic bird
61 species[28–30]. We extend the approach to a wild host-parasite system and their blood parasites to
62 identify genes involved in intra- and intercellular interactions between cells of both organisms. By
63 examining the extent of virulence elicited by the parasites, we highlight potential mechanisms driving
64 immunosuppression, increasing host tolerance and suppressing fitness costs.

65 Results

66 Identification of 22 distinct cell populations in *L. toddi*-infected peripheral blood

67 A total of 38295 cells were separately sequenced and analysed, resulting in the identification of 22
68 transcriptional clusters via dimensionality reduction of transcriptional profiles (Fig. 1A). A comparison
69 of three HP (high parasitaemia) with three LP (low parasitaemia) samples allowed identification of
70 infected cell profiles (Fig. 1B). The proportions of peripheral blood cell types diverged between blood
71 smear- and scRNA-seq-derived counts (Tab. S2), indicating a potential bias introduced during cell
72 preparation for scRNAseq (e.g., due to density gradient centrifugation). Overall, 28337 annotated and
73 712 unannotated genes were detected. Transcript diversity (Fig. S1A), expression levels (normalised
74 UMI counts; Fig. S1B) and proportion of mitochondrial and parasite transcripts (Fig. S1C-D, Fig. S2)
75 varied strongly between clusters.

76 **Absence of pronounced changes in immune cell populations**

77 Comparing HP versus LP, expectedly strong increases in gametocytes were accompanied by slightly
78 decreasing proportions most other cell types (Fig. 1). Signs of adaptive immunity activation, such as
79 clonal expansion of lymphoid cells, were absent. Strong decreases were observed in few cell types such
80 as heterophils and B cells. The increase observed for red blood cells is possibly due to variation during
81 extraction (see methods).

82 **Strong differential gene expression occurs in two parasite cell types**

83 Overall, 1138 parasite DEGs, 866 host DEGs and 29 unannotated DEGs were identified (Tab. S4; cut-off
84 value: p-value (adjusted) ≤ 0.05). Subsetting the strongest DEGs (cut-off values: p-value (adjusted) ≤
85 0.05; $\log_2$-FC (averaged) ≥ 1) limited the pool of genes to 360 DEGs under LP versus 1165 DEGs under
86 HP. In the following, gametocyte-infected cells will be referred to as developing gametocytes, micro-
87 and macrogametocytes for simplicity. The highest number of DEGs was found in microgametocytes
88 and developing gametocytes, while macrogametocytes and host cells generally expressed fewer DEGs
89 (Fig. S5A-C). Among gametocyte clusters, we observed more shared DEGs between microgametocytes
90 and developing gametocytes, than with macrogametocytes (Fig. 2A). Host DEGs were largely expressed
91 under LP, whereas parasite DEGs were predominantly present in HP samples (Fig. 2B, S5B & S5C). Since
92 parasite genes dominated under HP in developing gametocytes and the unannotated genes followed
93 the same trend, they likely represent parasitic transcripts. The strongest parasite DEGs were exclusive
94 to HP, but present in all host clusters. The strongest host DEGs were slightly more expressed under LP
95 than under HP. This implies an overall downregulation of host transcriptomic responses under HP.

96 A comparison of uninfected versus infected samples was not feasible due to the high prevalence of *L*.
97 *toddi* in the wild study population during sample acquisition. In order to validate that differential
98 expression analysis of HP versus LP groups represented changes in gene expression related to gradual
99 changes in parasitaemia, we correlated gene expression with parasitaemia (infection intensity) as a
100 continuous variable determined from blood smears. The analysis delivered fewer genes of interest

101 with a higher ratio of parasite to host genes. 216 CGs (correlated genes) showed a strong correlation
102 with parasitaemia (Tab. S5, cut-off value: FDR ≤ 0.05). In summary, 182 parasite and 34 host CGs were
103 correlated with the gradient of parasitaemia. The correlations were almost exclusively positive apart
104 from 4 host CGs displaying a negative correlation with parasitaemia in heterophils. Out of the 216 CGs
105 (Tab. S5) 19 parasite genes also represented DEGs retrieved by differential expression analysis (Tab.
106 S4; cut-off value: p-value (adjusted) ≤ 0.05).

107 **Cell-type specificity of DEGs**

108 While we expected to observe cell-type specific host DEGs, parasite gene expression might rely on a
109 more homogenous transcriptomic makeup across cell types, potentially required for the initial invasion
110 of host cells by merozoites. The redundancy of DEGs across clusters was therefore expectedly higher
111 for parasite than for host DEGs (Fig. S7). The most redundant parasite DEGs under HP were expressed
112 in host cells but not in gametocytes, further supporting their involvement in widescale invasion of host
113 cells by merozoites (Tab. 1, Fig. S7 & S5).

114 **Immune gene expression generally lacks correlation with parasitaemia**

115 The host immune genes which ranked among the top five DEGs were largely downregulated under HP
116 within various cell types (Tab. 1). These genes are implicated in processes such as in T cell activation,
117 the inflammatory response or pathogen defence (Tab. 1). The strong downregulation of immune genes
118 in various cell types indicates the absence of a pronounced immune response during increasing
119 parasitaemia, possibly due to immunosuppression.

120 Immune effectors including cytokines remained largely unaffected by increased parasitaemia or even
121 displayed downregulation across cell types. Cytokines are crucial for the vertebrate immune response
122 to pathogens[31]. While generally promoting parasite elimination, an exaggerated pro-inflammatory
123 response via TNF-α, IL-6, or IL-8 can also favour severe malaria and pathogenicity[32]. While mostly
124 displaying weak ubiquitous expression, certain cytokines were highly expressed in certain clusters

125 (Tab. S6), but not as significant DEGs (Tab. S6). As an exception, *TGF-β* displayed differential expression
126 under LP in thrombocytes and monocytes.

127 MHC-I components were upregulated under HP in thrombocytes, erythrocytes, T cells and eosinophils
128 (Tab. S6). In contrast, these genes were downregulated under HP in some B cells, T cells and in
129 monocytes (Tab. S6). Interestingly, microgametocytes displayed upregulation of *B2M* (MHC-I
130 component) under HP, while developing gametocytes exhibited the opposite pattern (Tab. S6). MHC-
131 II components were downregulated in some B cell clusters and monocytes under HP (Tab. S6).

132 Among the detectable immunoglobulin mRNAs only *IgL* (*Immunoglobulin light chain λ*) expressed in B
133 cells was significantly diminished under HP (Tab. S6).

134 **Opposing patterns of host gene expression in gametocyte subtypes**

135 PPI-network analysis of host DEGs was conducted to identify pathways responding to parasitaemia.
136 Focusing on developing gametocytes and microgametocytes showing the highest number of DEGs (Fig.
137 2), we retrieved networks with genes partially reoccurring in both clusters, but displaying opposite
138 expression patterns (Fig. 3). The largest group of such interactors were components of the ribosome
139 which were downregulated in developing gametocytes, but upregulated in microgametocytes under
140 HP (Fig. 3).

141 Discussion

142 This study is the first to perform scRNA-seq on a free-living avian host and its unculturable
143 haemosporidian parasite, demonstrating both the feasibility and opportunities of the method in
144 evolutionary ecology. We focused on changes of host responses to different levels of parasitaemia
145 which are informative about gene expression linked to the severity of infection. Which general
146 patterns can be observed and how do these responses differ between cell types?

147 The annotation of the clusters comprised of *Leucocytozoon toddi* gametocytes based on marker genes
148 led us to subdivide them into putative developing gametocytes, micro- and macrogametocytes. This

149 division is also suggested by the bifurcation of macro- and microgametocyte clusters from the
150 progenitor cell cluster, much like the pattern observed in *P. falciparum*[33]. It is striking that gametocyte
151 subtypes displayed strong differences with regard to basic cellular properties. While general transcript
152 abundance and the ratio of parasite versus host transcripts was highest in macrogametocytes, this
153 cluster simultaneously exhibited the lowest proportion of parasite mitochondrial gene transcripts. The
154 functional differences between micro- and macrogametocytes connected to these alterations in
155 transcript abundance might be linked to differing mitochondrial-to-nuclear genome ratios between
156 *Leucocytozoon* gametocyte types[34]. On the other hand, they are also reminiscent of a mechanism
157 described in *Plasmodium* where maternally derived mRNA-pools drive zygote development[35]. The
158 overall weak transferability of *Plasmodium* gametocyte markers is not surprising, given the estimated
159 phylogenetic distance of 46-74 million years between *Leucocytozoon* and other haemosporidians but
160 complicated the annotation[17]. Conversely, the synergy between our study and diverse scRNA-seq
161 studies on *Plasmodium* can inform about cellular markers and processes which are either common or
162 specific to different groups of blood parasites. For instance, a certain level of conservation between
163 mechanisms controlling macro- versus microgametocyte differentiation in *Plasmodium* and
164 *Leucocytozoon* appears to exist, since we identified an orthologue of *DOZI*, which functions as a
165 translational repressor in macrogametocytes of *Plasmodium*, as a marker of macrogametocytes[35].
166 With the help of such markers, gametocyte ratios might become estimable based on gross blood
167 transcriptomic data.

168 Classically, gametocytes of *Leucocytozoon* are thought to develop within erythroblasts, erythrocytes,
169 and mononuclear leukocytes[18]. On the other hand, it has more recently been suggested that some
170 *Leucocytozoon* species solely infect thrombocytes, while other species seem to differ in their host cell
171 choice[36–38].The overall similarity of transcriptional profiles between gametocytes and thrombocytes
172 which we show also points to thrombocytes as the preferred host cell type in buzzards. Thrombocytes
173 were clustered into four cellular subtypes. Whether these subtypes also display different functions and
174 host-parasite interactions remains to be investigated. Meanwhile, parasite transcripts were also

175 notably expressed at low levels in several host cell types. This global expression of parasite genes
176 across host cell types under HP might be due to a promiscuous invasion of host cells by merozoites
177 under HP. The upregulation of genes required for invasion of host cells by merozoites in *P. falciparum*
178 such as *PfIMC1i* and *G2* supports this interpretation[39]. We also observed an expression of different
179 host cell-type markers in different gametocyte subtypes, which might represent residual expression of
180 host genes after invasion or parasite-driven ectopic expression. Hence, parasite micro- and
181 macrogametocytes might each preferentially develop from different host peripheral blood cell types.
182 In conclusion, our data suggests thrombocytes as preferred host cell types of gametocytes, while low
183 level expression of parasite transcripts indicates a widescale invasion of diverse blood cell types under
184 HP.

185 We found that host transcriptional profiles differed strongly between parasitaemia levels. Cells
186 harbouring developing gametocytes, micro- and macrogametocytes partly even displayed opposing
187 trends. This finding indicates that developing versus differentiated gametocytes face – and in turn
188 shape – very different regulatory environments within their host cells. Firstly, the bulk of DEGs
189 occurred in developing gametocytes which indicates that transcriptional host-parasite interactions
190 might peak during the onset of parasite development, when interactions are first calibrated and the
191 intracellular niche is established[40]. In fact, the reprogramming and restructuring of the host cell is well
192 known to require and elicit profound transcriptional changes by intracellular protozoa[41,42].

193 Secondly, we detected opposing patterns of differential expression in the different gametocyte
194 subtypes. This pattern was mainly observed for genes involved in host ribosome biogenesis, a process
195 which is also known to enhance growth and proliferation during carcinogenesis if deregulated[43]. While
196 these genes were downregulated under HP in developing gametocytes, they were upregulated in
197 microgametocytes, and no pattern was observed in macrogametocytes. This could be explained by an
198 unknown density-dependent mechanism favouring host ribosome biogenesis in developing
199 gametocytes under low parasitaemia and in microgametocytes under high parasitaemia, which would
200 be absent in macrogametocytes. We also observed downregulation of host RNA metabolism,

201 indicating allocation or hijacking of resources towards parasitic gene expression. This was connected
202 with a deregulation of genes linked to the host's actin cytoskeleton and is known to occur during the
203 early development of other intracellular protists[44–46].

204 A first important finding supporting the idea of immunosuppression during *L. toddi* infection was the
205 absence of pronounced differences in immune cell populations depending on the level of parasitaemia.
206 Many other intracellular parasites have been shown to prevent activation and clonal expansion of T
207 cells and other immune cells required for parasite clearance[12–14]. Second, the majority of differentially
208 expressed host genes were downregulated under HP, further supporting the notion of
209 immunosuppression. Concomitantly, we also found several genes involved in the immune response to
210 be downregulated under HP across multiple cell types. This included downregulation of calgranulin-
211 and avidin-encoding genes in CD4+ T cells or *NOS2* in microgametocytes. In contrast to our
212 observations, these genes have been shown to be transcriptionally upregulated in response to LPS-
213 injection in wild passerines and upon *Salmonella enterica*-infection in chicken[47–49]. A second indication
214 of immunosuppression was provided by the downregulation of MHC-I and -II expression, which has
215 been characterised as a mechanism of immune evasion in *Leishmania donovani* and *Toxoplasma gondii*
216 infection[50–53]. While a similar mechanism might drive the downregulation of *B2M* in developing *L. toddi*
217 gametocytes under HP, it remains puzzling that we found the opposite effect in microgametocytes. On
218 the other hand, a wide range of host cell types also displayed upregulation of MHC-I components under
219 HP. However, MHC-I upregulation did not seem to evoke a strong CD8+ T cell response. This is
220 suggested by a lack of a pronounced cytokine response and downregulation of genes involved in CD8+
221 T cell activation. The weak and promiscuous expression patterns of various cytokines indicate an
222 overall mild inflammatory response regardless of infection intensity. Additionally, this response is
223 downregulated under HP in the case of *IL-8 like* and *TGF-β* in thrombocytes. While the upregulation of
224 *IL-8 like* under HP in eosinophils might contribute to the inflammatory response, this effect might be
225 neutralised by downregulation in thrombocytes. The lack of differential expression of *IL-2, IL-16, IL-18,*
226 *IL-7*, *IL-15, TNF11*, *TNF13B* and *TNF8-like* comparing between LP and HP does not indicate a correlation

227 with parasitaemia. The expression of these genes might either be constitutive or induced during the
228 onset of infection without further increase during the course of infection. Finally, the expression of
229 immunoglobulins remained stable or was even downregulated under HP, which is also in agreement
230 with the finding that antibody titres of buzzard nestlings could not be linked to *Leucocytozoon* infection
231 intensity in an earlier study by our group[54].

232 The widescale downregulation of several immune genes indicates the presence of immunosuppressive
233 effects under high *Leucocytozoon* infection intensity. As this pattern can result from the inter-
234 individual variation of host immunity and infection trajectories it would need to be addressed by
235 performing experimental infections. However, such experiments are both logistically and ethically
236 unfeasible with *Leucocytozoon* in protected free-living raptor hosts. For this purpose, other
237 comparable models would need to be developed. Thus, while we cannot be secure that widescale
238 downregulation of immune genes is the outcome of manipulation by the parasite, this interpretation
239 seems likely.

240 Within the various peripheral blood cell-types we observed highly cell-type specific transcriptional
241 responses to parasitaemia, some of which might be reactions to manipulation by the parasite. A vast
242 body of literature on comparable host-parasite systems suggests the functions of genes which exhibit
243 parasitaemia-related expression changes. Although these connections remain speculative, they can
244 help to understand how and which mechanisms utilised by other intracellular protozoa for host
245 manipulation might be at play in *Leucocytozoon*. Overall, we observed a repetitive pattern of cell-type
246 specific downregulation of immune-related DEGs under high parasite load in various host cell types.
247 On the other hand, certain DEGs identified in our analysis could confer tolerance to infection by
248 mitigating the effects of parasite growth and load, while others may promote parasite growth. An
249 example of cell-type specific immunosuppression could be provided by the downregulation of *DTNA*
250 and of *CCDC155* in CD4+ T cells potentially affecting T cell activation. DTNA is known as a component
251 of the DGC (dystrophin-glycoprotein complex) found in striated muscle cells[55]. CCDC155 has been
252 characterised as a component of the LINC (linkers of the nucleoskeleton to the cytoskeleton)-complex

253 coupling chromosomes to the cytoskeleton during meiosis[56]. Interestingly, immunological synapse
254 formation during T cell activation involves both the LINC-complex and the DGC[57,58]. T cell activation
255 might also be suppressed in CD8+ T cells, since some genes known to be involved in this process were
256 downregulated under HP. For instance, *TXNRD1* is upregulated during activation and clonal expansion
257 of T cells in response to *Leishmania major* infection[59]. Consequently, *TXNRD1*-deficiency leads to
258 increased parasitaemia[59]. In microgametocytes the downregulation of *NOS2* under HP might play a
259 role in increasing host tolerance to infection. Intracellular protists are known to downregulate iNOS as
260 a mechanism of immune evasion as exemplified by *T. gondii* and *L. amazonensis* infections[60,61].
261 Inducible nitric oxide synthase (iNOS) encoded by *NOS2* catalyses the production of anti-parasitic nitric
262 oxide (NO), which at excess causes cytotoxic damage to the host[62–64]. Therefore, a downregulation of
263 *NOS2* might be beneficial, especially under high parasite burden and highlights the possibility of a
264 mechanism enabling tolerance to infection. As an example of a gene potentially promoting parasite
265 growth, *FTH1,* encoding a subunit of ferritin required for iron sequestration was upregulated under HP
266 in thrombocytes. Ferritin confers tolerance to malaria in humans by preventing labile iron from
267 activating pro-apoptotic signalling pathways in hepatocytes[65]. However, this is unlikely to be needed
268 during *Leucocytozoon*-infections since they do not cause haemolysis and excessive release of iron as
269 seen in *Plasmodium*-infections[18]. A mechanism as observed in *Leishmania amazonensis*-infected
270 macrophages is more likely, where FTH1 promotes parasite growth through iron scavenging[66]. This
271 interpretation is further supported by the notion that *FTH1* was also upregulated in microgametocytes.

272 Our findings indicate that the low virulence of *L. toddi* is associated with widescale immunosuppression
273 in peripheral blood. At the same time, the sampled individuals might differ in their susceptibility to
274 infection or represent different time points of infection, which may also correspond to different
275 immunological responses. Immunosuppression can prevent excessive immune responses, which can
276 be damaging to the host (e. g. excessive cytokine production[42]). Therefore, the inhibition of such
277 pathways during parasitic infections can be beneficial to the host under certain circumstances such as
278 low parasite virulence. For instance, costs of infection may be resource-dependent and thus could be

279 compensated by additional food provisioning as long as buzzard nestlings are provided with parental
280 care[22]. Accordingly, recent findings show *Leucocytozoon* infection at the nestling stage is not predictive
281 of strong immediate pathology or later survival[23]. Immune evasion can have a mitigating effect on
282 virulence and in certain contexts assist the evolution of host tolerance[3]. Vector-mediated parent-to-
283 offspring transmission, i.e. quasi-vertical transmission, may facilitate the evolution towards low
284 virulence in *L. toddi*[67,68]. This pattern of transmission might be a pervasive consequence of social niche
285 choice, i.e., territoriality and local confinement of parents and offspring through extended parental
286 care leading to transmission[68,69].

287 In this light, our study starts to fill a big phylogenetic gap in the knowledge on molecular tools and
288 strategies used by blood parasites in the wild. It provides a rare example of reduced immunopathology
289 in an apparently highly co-adapted host-parasite-system elucidated down to the cellular and molecular
290 mechanisms. It therefore contributes a valuably detailed reference within a spectrum of strategies and
291 levels of host-parasite antagonism that still remains to be understood in the wild nature.

292 # Methods

293 **Sample acquisition and preparation**

294 Samples were collected in June 2021 in a population of Common Buzzards in eastern Westphalia,
295 Germany (8°25'E and 52°06'N). Occupied nests had previously been located in March and April. In a
296 first sampling event, blood samples were taken from the ulnar vein of nestlings. Air-dried blood smears
297 were prepared in the field, fixed in absolute ethanol and stained with Giemsa[18]. Parasitaemia of *L.*
298 *toddi* was estimated microscopically based on gametocyte counts. From this pool of sampled 345
299 buzzard nestlings from 164 territories, six individuals were chosen for further sampling based on their
300 infection status ("low" versus "high" parasitaemia; Tab. S1). Uninfected nestlings were not available
301 due to the extremely high prevalence of the parasite in the study population. Selected individuals
302 originated from six different breeding territories, which were evenly distributed throughout the study
303 area. In a second sampling event (maximum ten days after first sampling), three individuals with "low
304 parasitaemia" (LP: 0.017%, 0.025% & 0.133% of total blood cells) and three individuals with "high
305 parasitaemia" (HP: 0.956%, 1.384% & 1.699% of total blood cells) were brought to the Genomics &
306 Transcriptomics Laboratory of the Heinrich-Heine-University in Düsseldorf, Germany. A blood sample
307 with a volume of 1 mL was taken from the ulnar vein, transferred to a 15 mL centrifuge tube for Percoll
308 (Sigma-Aldrich) density gradient centrifugation with discontinuous layers of 55%, 45%, 35%, and 25%
309 solutions of stock isotonic Percoll (SIP) diluted with PBS at 7.4 pH. The density gradient centrifugation
310 was performed to deplete erythrocytes (swinging-bucket centrifuge rotor, 500 x g, 15min at 20°C). The
311 easily visible upper non-erythrocytic phases, containing larger and less dense cells compared to avian
312 erythrocytes, were extracted, and immediately subjected to single cell processing. Variation in the
313 extraction of leukocytes may cause differences in cell type proportions between samples as highly
314 infected samples have less discrete layering of cell types during density gradient centrifugation. For
315 comparison of cell type proportions with scRNA-seq all peripheral blood cell types were counted via
316 microscopy of blood smears. Per sample approximately 30000 cells were counted within 20 random
317 fields of view (Tab. S2). The nestlings were immediately returned to their nests after sampling and

318 transport. Sampling and transport of nestlings were permitted by the ethics commission of the Animal
319 Care and Use Committee of the German North Rhine-Westphalia State Office for Nature, Environment
320 and Consumer Protection (Landesamt für Natur, Umwelt und Verbraucherschutz Nordrhein-
321 Westfalen) under the reference number 84-02.04.2017.A147.

322 **Single Cell Library Generation**

323 A total of ~40,000 single cells were generated on the 10X Chromium Controller system for single-cell
324 droplet library generation utilizing the Chromium Single Cell 3' NextGEM Reagent Kit v3.1 (10X
325 Genomics, Pleasanton, CA, USA) according to manufacturer's instructions. Sequencing was carried out
326 on a NextSeq550 system (Illumina Inc. San Diego, USA) with a mean sequencing depth of ~50,000
327 reads/cell.

328 **Processing of 10X Genomics single cell data**

329 Raw sequencing data were processed using the 10X Genomics CellRanger software (v7.0). Raw BCL-
330 files were demultipexed and processed to Fastq-files using the CellRanger *mkfastq* pipeline. A custom
331 reference was created by combining draft *B. buteo* and *L. toddi* genomes using the cellranger *mkref*
332 pipeline. Alignment of reads to the genome and UMI (unique molecular identifier) counting was
333 performed via the CellRanger *count* pipeline to generate a gene-barcode matrix. All samples were
334 aggregated and normalised for sequencing depth using the cellranger *aggr* pipeline.

335 Further analyses were carried out with the Seurat v4.1.1 R package[70–72]. Initial quality control consisted
336 of removal of cells with fewer than 200 detected genes as well as removal of genes expressed in less
337 than three cells. Furthermore, cells with a mapping rate of > 10% to the mitochondrial genome were
338 removed, as they most likely represent dead or damaged cells. Cell doublets were removed from the
339 dataset using DoubletFinder v2.0[73]. Normalization was carried out utilizing SCTransform. Dimensional
340 reduction of the data set was achieved by Principal Component analysis (PCA), based on identified
341 variable genes and subsequent UMAP (Uniform Manifold Approximation and Projection) embedding.
342 The number of meaningful Principal Components (PC) was selected by ranking them according to the

343 percentage of variance explained by each PC, plotting them in an "Elbow Plot" and manually
344 determining the number of PCs that represent the majority of variance in the data set. Cells were
345 clustered using the graph-based clustering approach implemented in Seurat. Marker genes defining
346 each cluster (MGs) as well as differentially expressed genes (DEGs) comparing LP and HP nestlings were
347 calculated using a Wilcoxon Rank Sum test implemented in Seurat. Additionally, correlated gene
348 expression with parasitaemia determined by blood smear cell counts (see methods above) were
349 performed. Linear models were fitted to the averaged expression of each gene per cluster versus the
350 gradient of parasitaemia values to identify correlated genes (CGs). The false discovery rate was
351 calculated to account for multiple testing.

352 **Cluster annotation and downstream analyses**

353 Literature-curated markers were used to annotate Seurat clusters with avian peripheral blood cell
354 types and haemosporidian gametocyte stages (Fig. 1, S3 & S4). Blood cell markers from *Gallus gallus*
355 and *Plasmodium falciparum* (lineage 3D7) gametocyte markers were utilised[30,74–79]. The annotation of
356 cell types was further aided by the overall similarity of transcriptional profiles (Fig. 1A), marker genes
357 with indicative functions (MGs; Tab. S3) and parasite transcript abundance (Fig. S1D, Fig. S2). Multiple
358 clusters could be grouped into one cell type based on the expression of marker genes, while the
359 identity of subtypes remained elusive. Downstream analyses were performed using R version 4.1.2 for
360 data processing and exploration[80].

361 **Network analysis of DEGs**

362 Protein-protein-interaction (PPI) network analysis of host DEGs was conducted with Cytoscape
363 stringApp v2 using *Aquila chrysaetos chrysaetos* as reference species to generate networks based on
364 DEGs with cut-off values $p \geq 0.05$ (Bonferroni adjusted) and $\log_2$FC (averaged per cluster) ≥ 1[81–83]. Only
365 interactions with a confidence score of ≥ 0.9 were retrieved. Pathway enrichment analysis was
366 performed via the enrichment tool implemented in stringApp v2 using the referenced genome as a

background. For comparability, only enriched KEGG (Kyoto Encyclopedia of Genes and Genomes) pathways were highlighted.

Data and resource availability

The .fastq-files containing scRNA-seq sequences are deposited in the European Nucleotide Archive (ENA) at EMBL-EBI under accession number PRJEB73843. R-code for downstream analyses is accessible via Dryad (DOI: 10.5061/dryad.sbcc2frf2).

Acknowledgments

Sampling and processing of the samples was supported by the German Research Foundation (DFG), as part of the SFB TRR 212 (NC³) – project numbers 316099922 and 396780709 and DFG project number 398434413 to OK and NC. This work was also supported by the DFG Research Infrastructure West German Genome Center, project 407493903, as part of the Next Generation Sequencing Competence Network, project 423957469. Next Generation Sequencing and/or analyses was carried out at the West German Genome Center Düsseldorf. NC and OK received the DFG grant #DJ 154/4-4 as part of the DFG Sequencing call #2. Computational infrastructure and support were provided by the Centre for Information and Media Technology at Heinrich Heine University Düsseldorf and from the Center for Biotechnology, CeBiTec, Bielefeld University.

Author contributions

NC and OK designed the research. NC was involved in sample acquisition. NC and TL performed laboratory procedures. TL and TMR analysed the data. TMR wrote the paper. RP and JK provided critical feedback to the analyses and the manuscript.

387 # Tables and Figures

388 Table 1: Strongest DEGs across clusters (ordered by cell type). References indicate potential gene
389 functions. Immune genes upregulated under HP are indicated by "↑", whereas immunosuppression
390 (downregulation under HP) is indicated by "↓" (see column "Function").

Cluster	Para-sitemia	NCBI accession number	Gene	Ref. species	log_2-FC (avg.)	p-value (adj.)	Function	References
			Host					
9	HP	XP_031958267.1	*PHF10*	*Cm*	-1.36	1.65E-09	chromatin remodelling	85
	LP	XP_031970858.1	*TSSK6*	*Cm*	1.00	6.51E-06	chromatin remodelling	86
	LP	XP_040977087.1	*LOC121232750*	*Ac*	1.23	6.40E-06	-	-
	LP	XP_015480400.1	*MXD4*	*Pm*	1.86	5.18E-07	↓ blood progenitor proliferation, T cell survival	87,88
	LP	XP_029888348.1	*CDC42BPB*	*Ac*	2.14	6.93E-05	regulator of the cytoskeleton	89
0	HP	XP_029862693.1	*LOC115338306*	*Ac*	-1.11	4.05E-71	↑ MHC-I	90
	LP	XP_029877109.1	*ESAM*	*Ac*	1.49	1.16E-130	↓ neutrophil extravasation	91,92
1	HP	XP_029851964.1	*SYN2*	*Ac*	-2.03	2.68E-108	exocytosis	93–95
	LP	XP_040547522.1	*EYA1*	*Gg*	1.12	1.21E-68	DNA repair	96–98
	LP	XP_029877109.1	*ESAM*	*Ac*	1.41	1.11E-129	↓ neutrophil extravasation	91,92
3	HP	XP_029851964.1	*SYN2*	*Ac*	-2.14	5.52E-84	exocytosis	93–95
	HP	XP_029895765.1	*FTH1*	*Ac*	-1.01	1.17E-02	iron scavenging	65,66
	LP	XP_029859213.1	*MTMR12*	*Ac*	1.05	2.72E-21	endocytosis	99–101
	LP	XP_029852971.2	*ARHGAP36*	*Ac*	1.11	1.50E-51	neural development	102–104
	LP	XP_040547522.1	*EYA1*	*Gg*	1.16	2.01E-26	DNA repair	96–98
7	HP	XP_029851964.1	*SYN2*	*Ac*	-2.13	2.19E-81	exocytosis	93–95
	HP	XP_029866592.1	*PPDPF*	*Ac*	-1.29	5.16E-23	implicated in cancer progression	105,106
	LP	XP_029852971.2	*ARHGAP36*	*Ac*	1.10	1.28E-44	neural development	102–104
2	LP	XP_031953757.1	*CCDC155*	*Cm*	1.23	2.88E-89	↓ T cell activation	56,58
	LP	XP_018861179.1	*DTNA*	*Pm*	1.68	6.03E-162	↓ T cell activation	55,57
5	LP	XP_018861179.1	*DTNA*	*Pm*	1.04	8.17E-69	↓ T cell activation	55,57
8	LP	XP_018861179.1	*DTNA*	*Pm*	1.29	9.21E-67	↓ T cell activation	55,57
11	LP	XP_031953757.1	*CCDC155*	*Cm*	1.23	3.95E-17	↓ T cell activation	56,58
	LP	XP_018861179.1	*DTNA*	*Pm*	1.93	1.84E-40	↓ T cell activation	55,57
16	LP	XP_029861532.1	*LOC115337405*	*Ac*	1.32	7.03E-06	↓ anti-pathogenic	107
	LP	XP_029879656.2	*LOC115345306*	*Ac*	1.45	1.68E-04	↓ pro-inflammatory	108
18	LP	XP_029896238.1	*TXNRD1*	*Ac*	1.62	2.97E-11	↓ T cell activation	59
	LP	XP_029886923.1	*ALOX5*	*Ac*	1.63	3.08E-10	↓ T cell activation, inflammation & cell death	109–111
	LP	XP_018861179.1	*DTNA*	*Pm*	1.68	1.79E-08	↓ T cell activation	55,57
19	LP	XP_040977722.1	*LOC115337909*	*Ac*	1.01	1.04E-07	↓ T cell activation (putative)	112
	LP	XP_018861179.1	*DTNA*	*Pm*	1.02	1.57E-05	↓ T cell activation	55,57
	LP	XP_031953757.1	*CCDC155*	*Cm*	1.11	3.28E-05	↓ T cell activation	56,58
10	LP	XP_029881352.1	*S100A10*	*Ac*	1.44	1.25E-16	↓ pro-inflammatory	113
12	HP	XP_040977087.1	*LOC121232750*	*Ac*	-1.05	2.52E-44	-	-
	LP	XP_029862549.1	*LOC115338209*	*Ac*	1.19	6.80E-65	↓ MHC-II	51,53
4	HP	XP_029897790.1	*F13A1*	*Ac*	-1.19	3.19E-25	coagulation factor	114
	LP	XP_029861378.1	*ANXA1*	*Ac*	1.11	2.52E-27	↓ neutrophil extravasation	115
	LP	XP_029879656.2	*LOC115345306*	*Ac*	2.90	3.09E-48	↓ pro-inflammatory	108
13	HP	XP_040978593.1	*CSRNP1*	*Ac*	-1.05	7.52E-16	↑ immune cell growth & development	116
	LP	XP_029897792.1	*LY86*	*Ac*	1.03	1.33E-10	↓ regulator of Toll-Signalling	117
15	LP	XP_029871069.1	*LOC115341780*	*Ac*	2.71	9.06E-07	↓ anti-pathogenic (putative)	118
20	HP	XP_029893214.2	*FAM184A*	*Ac*	-1.39	6.19E-03	associated with human malignancies	119–121
6	HP	XP_029895765.1	*FTH1*	*Ac*	-2.67	1.90E-13	iron scavenging	65,66
	HP	XP_029893758.1	*LOC115351288*	*Ac*	-2.30	6.81E-08	antioxidant	122
	HP	XP_040977744.1	*LOC121233102*	*Ac*	-2.02	3.62E-09	carcinogenesis (putative)	123
	HP	XP_031957654.1	*RPS12*	*Cm*	-1.98	2.18E-09	ribosome	43
	HP	XP_029860305.1	*EMC4*	*Ac*	-1.89	6.82E-08	protein folding	124,125
	LP	XP_029890446.1	*LOC115349840*	*Ac*	3.88	3.78E-04	↓ anti-pathogenic (putative)	126–128
	LP	XP_029863942.1	*XRCC2*	*Ac*	4.01	1.84E-22	DNA repair	129,130
	LP	XP_029856482.1	*BTG2*	*Ac*	4.28	1.15E-13	↓ pleiotropic tumour suppressor gene	131,132
	LP	XP_029883424.1	*NOS2*	*Ac*	5.76	6.91E-26	↓ anti-pathogenic	62–64
	LP	XP_029871871.1	*PRKCQ*	*Ac*	6.47	8.03E-178	↓ T cell & platelet activation	133
17	LP	XP_029854753.1	*PRKD1*	*Ac*	3.95	5.47E-29	↓ T cell activation, pro-inflammatory	134,135
	LP	XP_040980327.1	*ARHGAP15*	*Ac*	4.09	1.57E-06	regulator of the cytoskeleton	136
	LP	XP_029883957.1	*VEZF1*	*Ac*	4.25	3.79E-21	↓ septic shock	137,138
	LP	XP_029863942.1	*XRCC2*	*Ac*	4.62	1.63E-19	DNA repair	129,130
	LP	XP_029888348.1	*CDC42BPB*	*Ac*	4.84	1.63E-24	regulator of the cytoskeleton	89
			Parasite					
9	HP	XP_024329154.1	*PF3D7_1214500*	*Pf*	-3.20	1.34E-51	enriched in gametocytes	139
	HP	XP_002585477.1	*PF3D7_1466500*	*Pf*	-2.93	1.04E-32	-	-
	HP	XP_002809016.1	*PF3D7_1316300*	*Pf*	-2.81	2.06E-33	-	-
	HP	XP_001349289.1	*PfIMC1i (PF3D7_0823500)*	*Pf*	-2.75	2.72E-36	morphological changes	39
	HP	XP_001350486.1	*Pf41-3 precursor (PF3D7_1207700)*	*Pf*	-2.58	1.53E-23	enriched in gametocytes	139
0	HP	XP_001349289.1	*PfIMC1i (PF3D7_0823500)*	*Pf*	-4.02	0.00E+00	morphological changes	39
	HP	XP_024329154.1	*PF3D7_1214500*	*Pf*	-3.94	0.00E+00	enriched in gametocytes	139
	HP	XP_002809016.1	*PF3D7_1316300*	*Pf*	-3.47	0.00E+00	-	-
	HP	XP_001348354.1	*PfPLC6 (PF3D7_1418300)*	*Pf*	-3.36	0.00E+00	host cell invasion (putative)	140,141
	HP	XP_002585477.1	*PF3D7_1466500*	*Pf*	-3.28	0.00E+00	-	-

Cluster	Para-sitemia	NCBI accession number	Gene	Ref. species	log_2-FC (avg.)	p-value (adj.)	Function	References
1	HP	XP_001349289.1	*PfIMC1i (PF3D7_0823500)*	*Pf*	-4.09	0.00E+00	morphological changes	39
	HP	XP_024329154.1	*PF3D7_1214500*	*Pf*	-3.90	0.00E+00	enriched in gametocytes	139
	HP	XP_002809016.1	*PF3D7_1316300*	*Pf*	-3.39	0.00E+00	-	-
	HP	XP_001348354.1	*PfPLC6 (PF3D7_1418300)*	*Pf*	-3.29	0.00E+00	host cell invasion (putative)	140,141
	HP	XP_002808700.1	*PfPSOP13 (PF3D7_0518800)*	*Pf*	-3.21	0.00E+00	host-to-vector transmission	142
3	HP	XP_001349289.1	*PfIMC1i (PF3D7_0823500)*	*Pf*	-4.19	0.00E+00	morphological changes	39
	HP	XP_024329154.1	*PF3D7_1214500*	*Pf*	-4.10	0.00E+00	enriched in gametocytes	139
	HP	XP_002809016.1	*PF3D7_1316300*	*Pf*	-3.53	0.00E+00	-	-
	HP	XP_001352166.1	*PF3D7_0929600*	*Pf*	-3.52	3.41E-294	morphological changes (putative)	39
	HP	XP_001348354.1	*PfPLC6 (PF3D7_1418300)*	*Pf*	-3.51	1.17E-281	host cell invasion (putative)	140,141
7	HP	XP_001349289.1	*PfIMC1i (PF3D7_0823500)*	*Pf*	-3.93	1.33E-231	morphological changes	39
	HP	XP_024329154.1	*PF3D7_1214500*	*Pf*	-3.77	1.32E-260	enriched in gametocytes	139
	HP	XP_002585477.1	*PF3D7_1466500*	*Pf*	-3.12	5.77E-159	-	-
	HP	XP_002809016.1	*PF3D7_1316300*	*Pf*	-3.10	1.10E-170	-	-
	HP	XP_001348354.1	*PfPLC6 (PF3D7_1418300)*	*Pf*	-3.06	2.76E-145	host cell invasion (putative)	140,141
2	HP	XP_024329154.1	*PF3D7_1214500*	*Pf*	-2.73	0.00E+00	enriched in gametocytes	139
	HP	XP_001349289.1	*PfIMC1i (PF3D7_0823500)*	*Pf*	-2.22	0.00E+00	morphological changes	39
	HP	XP_002809016.1	*PF3D7_1316300*	*Pf*	-2.08	0.00E+00	-	-
	HP	XP_001352166.1	*PF3D7_0929600*	*Pf*	-1.90	1.09E-296	morphological changes (putative)	39
	HP	XP_002585477.1	*PF3D7_1466500*	*Pf*	-1.89	3.03E-265	-	-
5	HP	XP_024329154.1	*PF3D7_1214500*	*Pf*	-2.39	0.00E+00	enriched in gametocytes	139
	HP	XP_001349289.1	*PfIMC1i (PF3D7_0823500)*	*Pf*	-1.81	1.88E-269	morphological changes	39
	HP	XP_002809016.1	*PF3D7_1316300*	*Pf*	-1.71	1.89E-255	-	-
	HP	XP_002585477.1	*PF3D7_1466500*	*Pf*	-1.67	2.83E-243	-	-
	HP	XP_001352166.1	*PF3D7_0929600*	*Pf*	-1.62	9.67E-253	morphological changes (putative)	39
8	HP	XP_024329154.1	*PF3D7_1214500*	*Pf*	-2.21	1.52E-263	enriched in gametocytes	139
	HP	XP_001349289.1	*PfIMC1i (PF3D7_0823500)*	*Pf*	-1.71	2.97E-189	morphological changes	39
	HP	XP_002809016.1	*PF3D7_1316300*	*Pf*	-1.51	1.26E-191	-	-
	HP	XP_001352166.1	*PF3D7_0929600*	*Pf*	-1.46	8.34E-183	morphological changes (putative)	39
	HP	XP_002585477.1	*PF3D7_1466500*	*Pf*	-1.34	1.26E-170	-	-
11	HP	XP_024329154.1	*PF3D7_1214500*	*Pf*	-4.12	2.69E-164	enriched in gametocytes	139
	HP	XP_001349289.1	*PfIMC1i (PF3D7_0823500)*	*Pf*	-3.63	1.19E-131	morphological changes	39
	HP	XP_002809016.1	*PF3D7_1316300*	*Pf*	-3.28	3.98E-107	-	-
	HP	XP_002585477.1	*PF3D7_1466500*	*Pf*	-3.20	1.04E-105	-	-
	HP	XP_002808700.1	*PfPSOP13 (PF3D7_0518800)*	*Pf*	-2.98	7.70E-101	host-to-vector transmission	142
16	HP	XP_024329154.1	*PF3D7_1214500*	*Pf*	-1.90	8.40E-78	enriched in gametocytes	139
	HP	XP_001349289.1	*PfIMC1i (PF3D7_0823500)*	*Pf*	-1.38	6.61E-50	morphological changes	39
	HP	XP_001348354.1	*PfPLC6 (PF3D7_1418300)*	*Pf*	-1.28	8.83E-66	host cell invasion (putative)	140,141
	HP	XP_002809016.1	*PF3D7_1316300*	*Pf*	-1.24	1.64E-63	-	-
	HP	XP_001352166.1	*PF3D7_0929600*	*Pf*	-1.15	1.11E-54	morphological changes (putative)	39
18	HP	XP_024329154.1	*PF3D7_1214500*	*Pf*	-3.09	1.80E-50	enriched in gametocytes	139
	HP	XP_001349289.1	*PfIMC1i (PF3D7_0823500)*	*Pf*	-2.55	3.51E-36	morphological changes	39
	HP	XP_002809016.1	*PF3D7_1316300*	*Pf*	-2.18	4.20E-37	-	-
	HP	XP_002585477.1	*PF3D7_1466500*	*Pf*	-2.16	3.52E-31	-	-
	HP	XP_001352166.1	*PF3D7_0929600*	*Pf*	-2.13	1.44E-37	morphological changes (putative)	39
19	HP	XP_001350425.1	*PfNEK3 (PF3D7_1201600)*	*Pf*	-2.11	5.74E-07	cell cycle regulation	143
	HP	XP_024329154.1	*PF3D7_1214500*	*Pf*	-2.09	9.48E-36	enriched in gametocytes	139
	HP	XP_001349289.1	*PfIMC1i (PF3D7_0823500)*	*Pf*	-1.54	4.42E-20	morphological changes	39
	HP	XP_002809016.1	*PF3D7_1316300*	*Pf*	-1.50	1.24E-27	-	-
	HP	XP_002585477.1	*PF3D7_1466500*	*Pf*	-1.36	2.19E-22	-	-
10	HP	XP_024329154.1	*PF3D7_1214500*	*Pf*	-2.90	8.26E-171	enriched in gametocytes	139
	HP	XP_002809016.1	*PF3D7_1316300*	*Pf*	-2.68	4.27E-128	-	-
	HP	XP_001350486.1	*Pf41-3 precursor (PF3D7_1207700)*	*Pf*	-2.60	1.04E-90	enriched in gametocytes	139
	HP	XP_001350425.1	*PfNEK3 (PF3D7_1201600)*	*Pf*	-2.54	1.50E-48	cell cycle regulation	143
	HP	XP_002585477.1	*PF3D7_1466500*	*Pf*	-2.43	6.87E-96	-	-
12	HP	XP_024329154.1	*PF3D7_1214500*	*Pf*	-2.05	8.31E-127	enriched in gametocytes	139
	HP	XP_001350486.1	*Pf41-3 precursor (PF3D7_1207700)*	*Pf*	-1.96	7.91E-58	enriched in gametocytes	139
	HP	XP_002585477.1	*PF3D7_1466500*	*Pf*	-1.82	3.86E-71	-	-
	HP	XP_002809016.1	*PF3D7_1316300*	*Pf*	-1.80	1.66E-79	-	-
	HP	XP_001352166.1	*PF3D7_0929600*	*Pf*	-1.69	1.99E-96	morphological changes (putative)	39
21	HP	XP_024329154.1	*PF3D7_1214500*	*Pf*	-1.27	2.40E-11	enriched in gametocytes	139
4	HP	XP_024329154.1	*PF3D7_1214500*	*Pf*	-4.05	0.00E+00	enriched in gametocytes	139
	HP	XP_002809016.1	*PF3D7_1316300*	*Pf*	-3.45	0.00E+00	-	-
	HP	XP_001349289.1	*PfIMC1i (PF3D7_0823500)*	*Pf*	-3.43	0.00E+00	morphological changes	39
	HP	XP_002585477.1	*PF3D7_1466500*	*Pf*	-3.25	0.00E+00	-	-
	HP	XP_001352166.1	*PF3D7_0929600*	*Pf*	-3.24	0.00E+00	morphological changes (putative)	39
13	HP	XP_024329154.1	*PF3D7_1214500*	*Pf*	-2.63	1.65E-133	enriched in gametocytes	139
	HP	XP_001349289.1	*PfIMC1i (PF3D7_0823500)*	*Pf*	-2.26	3.82E-111	morphological changes	39

Cluster	Para-sitemia	NCBI accession number	Gene	Ref. species	log_2-FC (avg.)	p-value (adj.)	Function	References
	HP	XP_002809016.1	*PF3D7_1316300*	*Pf*	-2.18	1.17E-95	-	-
	HP	XP_002585477.1	*PF3D7_1466500*	*Pf*	-2.07	1.95E-88	-	-
	HP	XP_001352166.1	*PF3D7_0929600*	*Pf*	-2.04	4.98E-88	morphological changes (putative)	[39]
15	HP	XP_024329154.1	*PF3D7_1214500*	*Pf*	-3.15	5.74E-64	enriched in gametocytes	[139]
	HP	XP_001350486.1	*Pf41-3 precursor (PF3D7_1207700)*	*Pf*	-2.94	1.84E-35	enriched in gametocytes	[139]
	HP	XP_002809016.1	*PF3D7_1316300*	*Pf*	-2.85	1.00E-41	-	-
	HP	XP_002585477.1	*PF3D7_1466500*	*Pf*	-2.67	6.10E-41	-	-
	HP	XP_001352166.1	*PF3D7_0929600*	*Pf*	-2.53	2.39E-56	morphological changes (putative)	[39]
20	HP	XP_002809016.1	*PF3D7_1316300*	*Pf*	-3.04	5.49E-18	-	-
	HP	XP_001349289.1	*PfIMC1i (PF3D7_0823500)*	*Pf*	-3.01	8.78E-19	morphological changes	[39]
	HP	XP_024329154.1	*PF3D7_1214500*	*Pf*	-2.94	1.38E-19	enriched in gametocytes	[139]
	HP	XP_001352166.1	*PF3D7_0929600*	*Pf*	-2.80	1.01E-17	morphological changes (putative)	[39]
	HP	XP_001348354.1	*PfPLC6 (PF3D7_1418300)*	*Pf*	-2.67	6.73E-17	host cell invasion (putative)	[140,141]
6	HP	XP_012769598.1	*BBBOND_0313150*	*Bb*	-2.91	5.00E-13	ABC-transporter	[144]
	HP	XP_001348212.1	*PF3D7_1404200*	*Pf*	-2.75	1.11E-12	-	-
	HP	XP_001349319.1	*PF3D7_0820600*	*Pf*	-2.63	2.72E-12	apicoplast (putative)	[145]
	HP	XP_001348354.1	*PfPLC6 (PF3D7_1418300)*	*Pf*	-2.56	7.22E-10	host cell invasion (putative)	[140,141]
	HP	XP_001348121.1	*PfRPS21 (PF3D7_1144000)*	*Pf*	-2.46	1.03E-09	ribosome	[146]
	LP	XP_001349989.1	*PfLDH (PF3D7_1324900)*	*Pf*	2.46	5.45E-10	lactic acid fermentation	[147,148]
	LP	XP_001347965.1	*PfPFK11 (PF3D7_1128300)*	*Pf*	2.88	2.15E-44	enriched in gametocytes	[149]
	LP	XP_001351121.1	*PfGLP1 (PF3D7_0304500)*	*Pf*	3.31	3.56E-12	glutaredoxin	[150]
14	LP	XP_002585462.1	*PfRPA3 (PF3D7_1442100)*	*Pf*	1.70	6.96E-03	DNA repair	[151]
	LP	XP_001350447.1	*PfUBC (PF3D7_1203900)*	*Pf*	2.30	1.02E-03	protein degradation	[152]
17	HP	XP_001350425.1	*PfNEK3 (PF3D7_1201600)*	*Pf*	-6.49	1.25E-29	cell cycle regulation	[143]
	HP	XP_001349778.1	*PfApiAP2 (PF3D7_1305200)*	*Pf*	-5.43	2.50E-23	repressed in macrogametocytes	[35]
	HP	XP_001349787.1	*PF3D7_1306000*	*Pf*	-5.00	2.24E-14	-	-
	HP	XP_966163.1	*PfH2A (PF3D7_0617800)*	*Pf*	-4.76	9.46E-34	histone protein	[153]
	HP	XP_002808835.1	*PfPPM5 (PF3D7_0810300)*	*Pf*	-4.71	5.84E-27	oocyst development	[154]

391

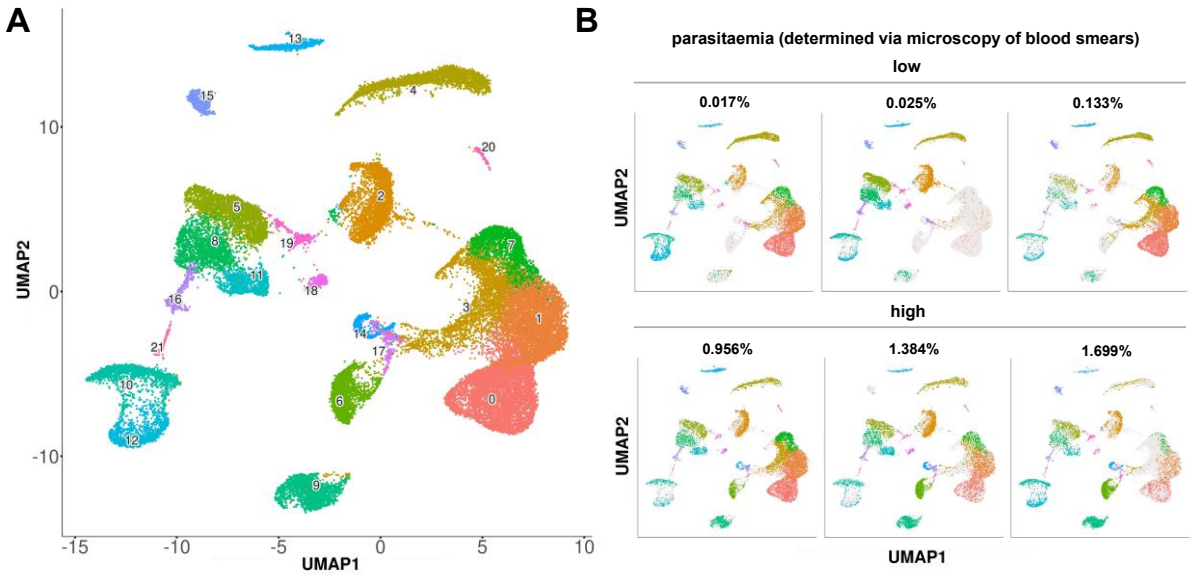

C

cluster	annotation	total relative abundance	parasitaemia (via blood smears) 0.017%	0.025%	0.133%	0.956%	1.384%	1.699%
			relative abundance per sample					
9	erythrocytes	0.049	0.005	0.016	0.012	0.046	0.100	0.141
0	thrombocytes	0.145	0.195	0.004	0.255	0.184	0.094	0.072
1		0.136	0.182	0.005	0.208	0.182	0.109	0.069
3		0.080	0.094	0.013	0.144	0.120	0.049	0.016
7		0.052	0.054	0.000	0.078	0.086	0.046	0.019
2	CD4+ T cells	0.084	0.044	0.205	0.037	0.067	0.108	0.074
5		0.068	0.058	0.181	0.023	0.047	0.061	0.064
8		0.049	0.038	0.129	0.015	0.036	0.047	0.050
11		0.032	0.020	0.069	0.012	0.023	0.054	0.022
16		0.014	0.010	0.037	0.005	0.010	0.017	0.009
18	CD8+ T cells	0.009	0.003	0.028	0.002	0.008	0.013	0.005
19		0.009	0.005	0.024	0.005	0.004	0.007	0.013
10	B cells	0.040	0.044	0.071	0.022	0.019	0.035	0.071
12		0.029	0.063	0.036	0.018	0.010	0.008	0.050
21		0.003	0.003	0.004	0.002	0.001	0.003	0.005
4	putative heterophils	0.078	0.146	0.097	0.093	0.050	0.052	0.017
13	putative eosinophils	0.026	0.013	0.050	0.029	0.037	0.014	0.010
15	putative monocytes	0.014	0.009	0.022	0.017	0.015	0.001	0.023
20	unannotated	0.005	0.006	0.002	0.014	0.005	0.002	0.001
6	putative microgametocytes	0.053	0.001	0.000	0.004	0.033	0.130	0.188
14	putative macrogametocytes	0.016	0.000	0.000	0.003	0.011	0.037	0.055
17	putative developing gametocytes	0.010	0.007	0.008	0.004	0.007	0.013	0.025

Figure 1: Overview of scRNA-seq clusters (Seurat clusters) and their proportions. (A) UMAP of 22 identified clusters. (B) Comparison of 6 samples categorised into LP versus HP based on their parasitaemia quantified via microscopy of blood smears. (C) Relative abundance of cell types comparing samples ordered by parasitaemia as quantified via microscopy of blood smears. Abundance is colour-coded by a red colour scale (normalisation per row).

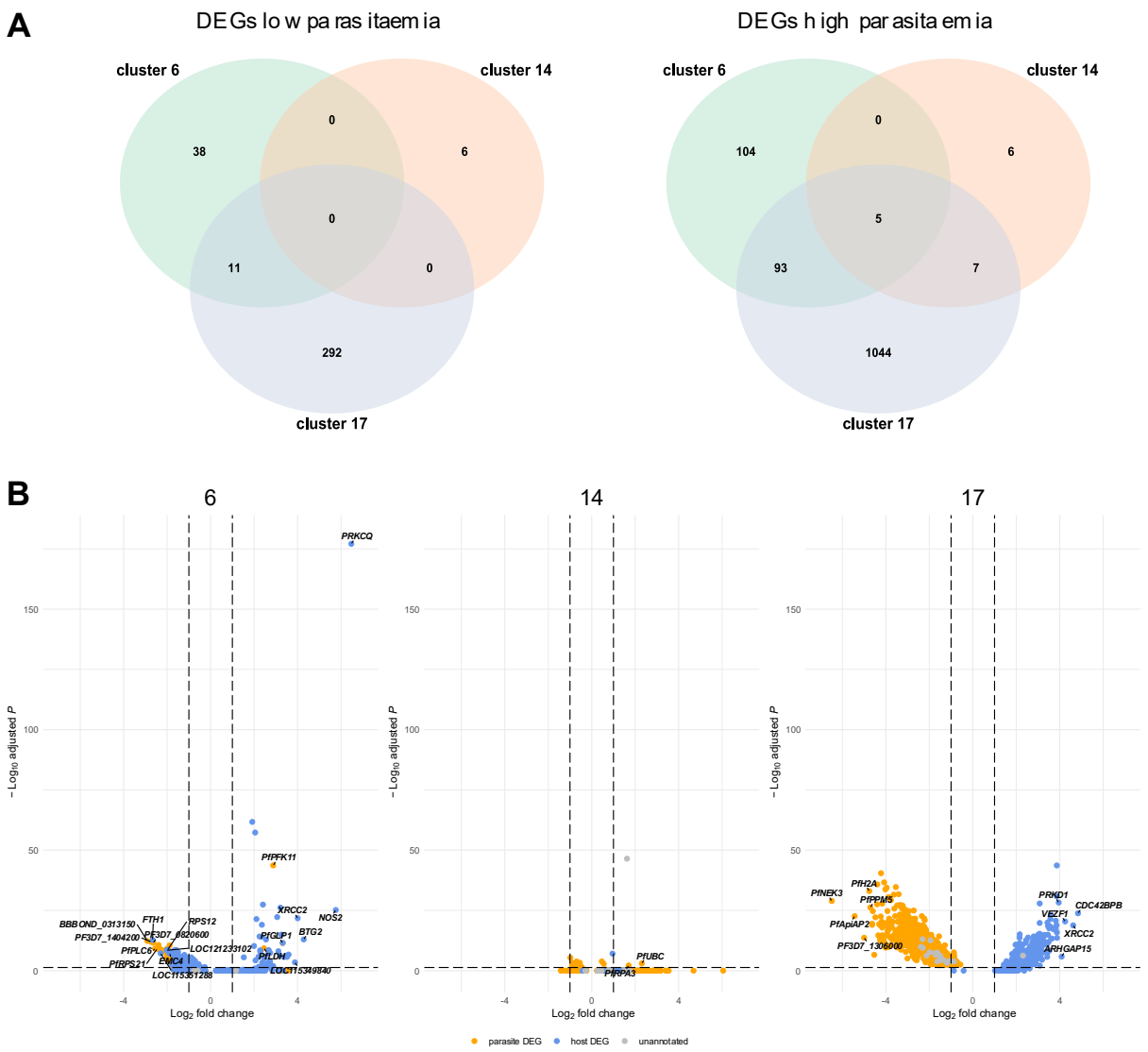

Figure 2: (A) Venn diagrams of DEGs in gametocyte clusters comparing LP and HP (cut-off: p-value (adjusted) ≤ 0.05). (B) Differential gene expression across gametocyte clusters (top five host and parasite DEGs of LP versus HP are labelled). Dotted lines delimit cut-off-values (p-value (adjusted) ≤ 0.05; log_2-FC (averaged) ≥ 1). Negative and positive values for log_2-FC represent differential expression under HP versus LP respectively.

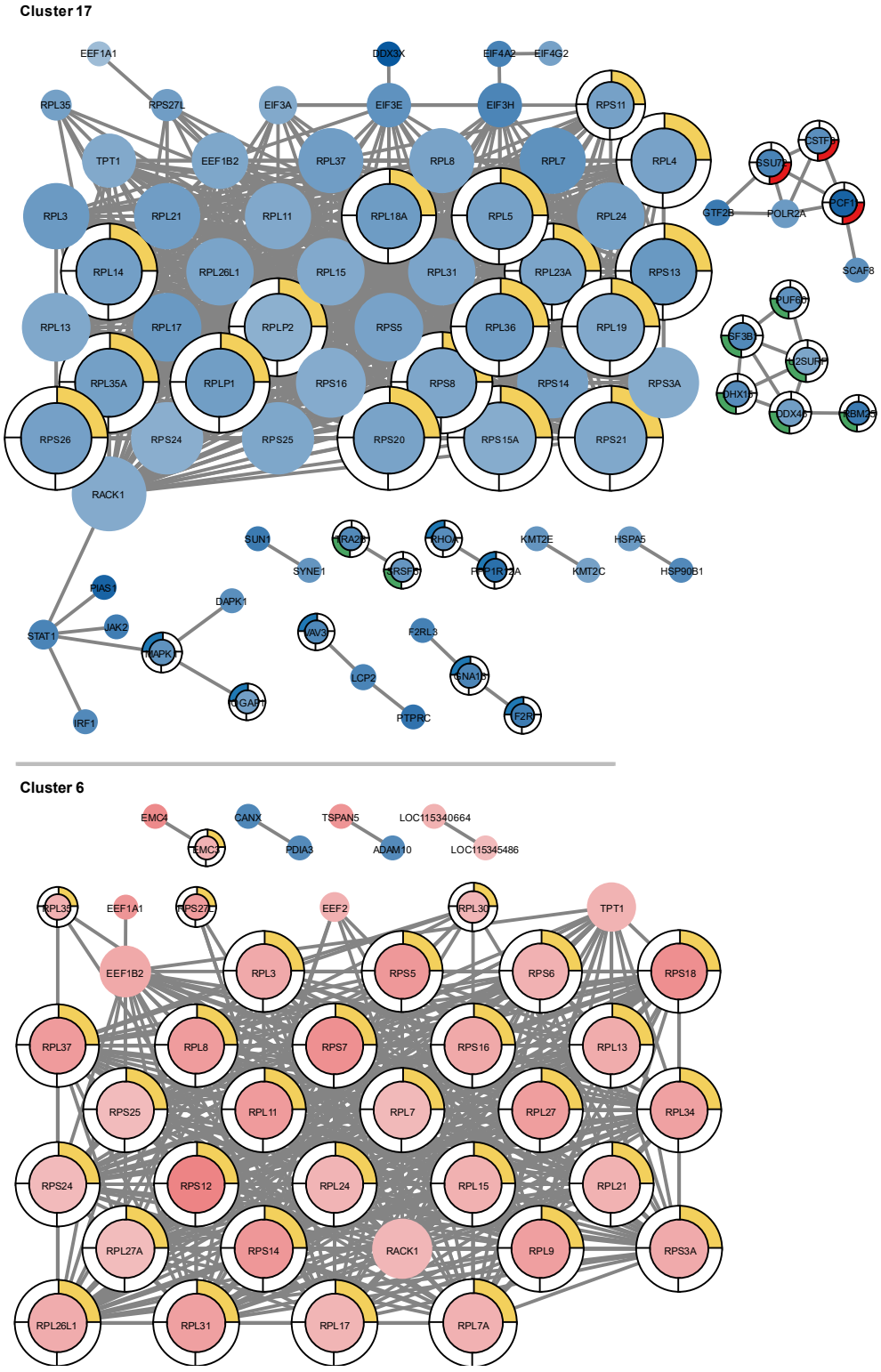

Figure 3: String PPI-networks of host genes (p-value (adjusted) ≤ 0.05; $\log_2$-FC (averaged) ≥ 1) of developing gametocytes microgametocytes. Node colour intensity encodes differential expression comparing LP (blue) versus HP (red). Colouring outside nodes refers to enriched KEGG pathways

409 (yellow: “ribosome” (False discovery rate (FDR) = 4.99E-36); red: “mRNA surveillance pathway” (FDR =

410 0.0451); green: “spliceosome” (FDR = 0.0047); blue: “regulation of actin cytoskeleton” (FDR = 0.0013)).

411 Node size corresponds to number of connections.

412 ## Extended Data Figures

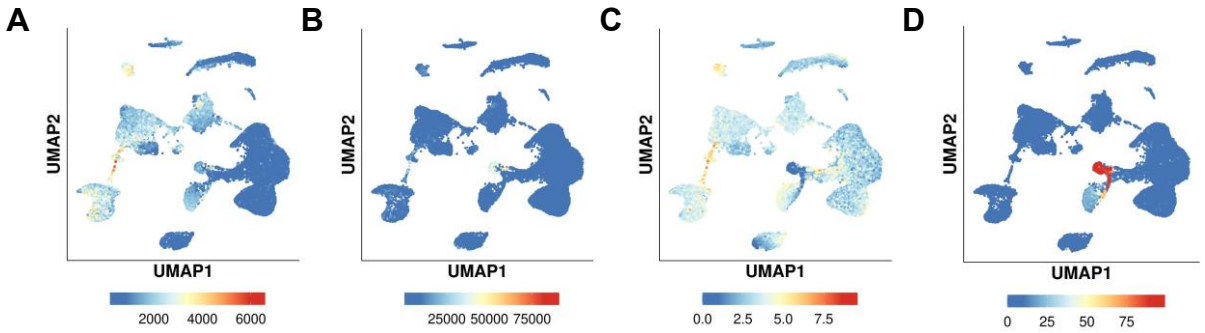

413

414 Figure S1: UMAPs displaying (A) number of genes expressed per cell, (B) number of UMIs detected per

415 cell, (C) proportion of mitochondrial genes per cell and (D) proportion of parasite genes per cell (genes

416 mapped to reference genomes of parasite species).

417

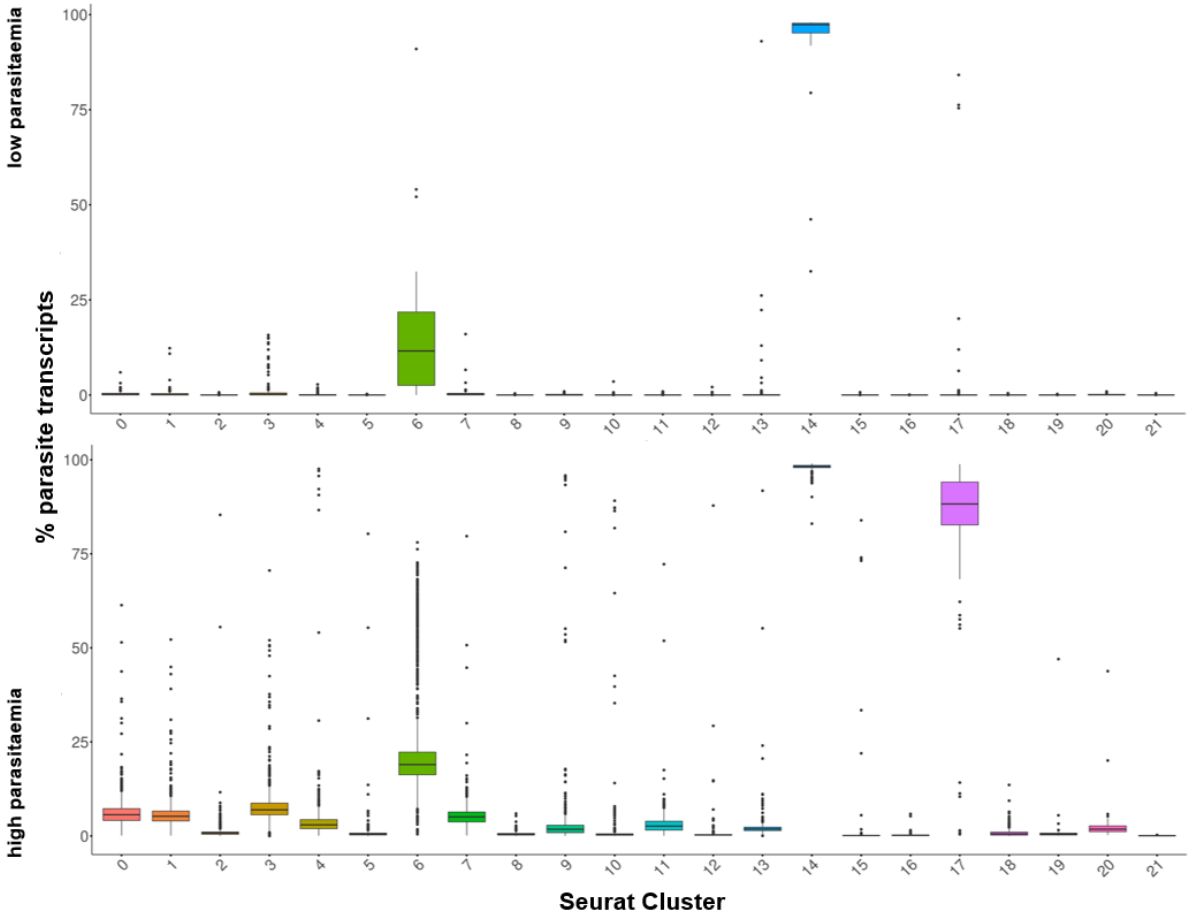

418

419 Figure S2: Proportion of parasite transcripts per cluster comparing low versus high parasitaemia.

420

Marker References
Cluster
red blood cells
thrombocytes
CD4+ T cell
CD8+ T cell
B cell
put. heterophil
put. eosinophil
put. monocyte
unannotated
put. microgametocyte
put. macrogametocyte
put. dev. gametocyte
9 0 1 3 7 2 5 8 11 16 18 19 10 12 21 4 13 15 20 6 14 17
[73]
Hemoglobin subunit α-A9
Hemoglobin subunit α-D9
Hemoglobin subunit β9
[74]
MPL (isoform X2)1, 3, 7
MPL (isoform X7)
GP9 7
ITGB30, 1, 3, 7
ITGB10, 1, 3, 7, 18
ITGA61, 3, 7
ITGA21, 3, 7
ITGAV4, 8, 11, 12, 13, 15, 16, 18, 20
F2R1, 3, 7
F2RL30, 1, 3, 7
P2RX1
P2RY1
HTR2A1, 6, 7
CD36
TBXAS11, 3, 4, 7, 13
GP1BA
[33]
CD3D2, 5, 8, 10, 11, 16, 18, 19
CD45, 8, 11, 16
IL7R2, 5, 8, 11, 19
CD285, 8, 16
CD8B18, 19
CD5
CD442, 4, 5, 8, 11, 13, 15, 16, 18, 19
BCL11A10, 12, 21
LOC115338201 10, 12, 15, 21
LOC115338202 10, 12, 15, 21
[76-77]
LOC115340258 (IL-8-like)
LOC115340259 (IL-8-like)1, 4, 7, 13, 15
IL18
GAL1
GAL313
GAL3
GAL7
LOC116441978 (GAL8-like)
GAL9
CTSB15
CTSD2, 4, 8, 12, 13, 15, 16, 18
CTSE
LOC115336252 (CTSEA-like)
CTSH12, 15
CTSK
CTSL
LOC115349310 (CTSL-like)4, 13, 18
CTSO
LOC115345557 (CTSS-like)15
CTSZ
LOC115334616 (LYZ-G-like)
LOC115334657 (LYZ-G-like, partial)15
LOC115334707 (LYZ-G-like)
ACP2
ACP3
ACP5
ACP6
GUSB15
GAA
LOC115335647 (GAA-like)
LOC115335647 (GAA-like)
GANC
GANAB
Percent Expressed
0
25
50
75
Average Expression
6
4
2
0

422 Figure S3: Dotplot of host marker genes curated from literature[30,76–80]. Clusters were *o*rdered by
423 qualitative examination of marker gene expression under consideration of cluster distribution in Fig.
424 1A. Final annotations are indicated at the top of the plot. Annotations in superscript list clusters in
425 which a gene is differentially expressed in comparison to all clusters. Gene names in grey font
426 represent indirectly inferred markers (non-transcriptomic markers). Duplicates are based on two
427 transcript variants mapped to the same gene.

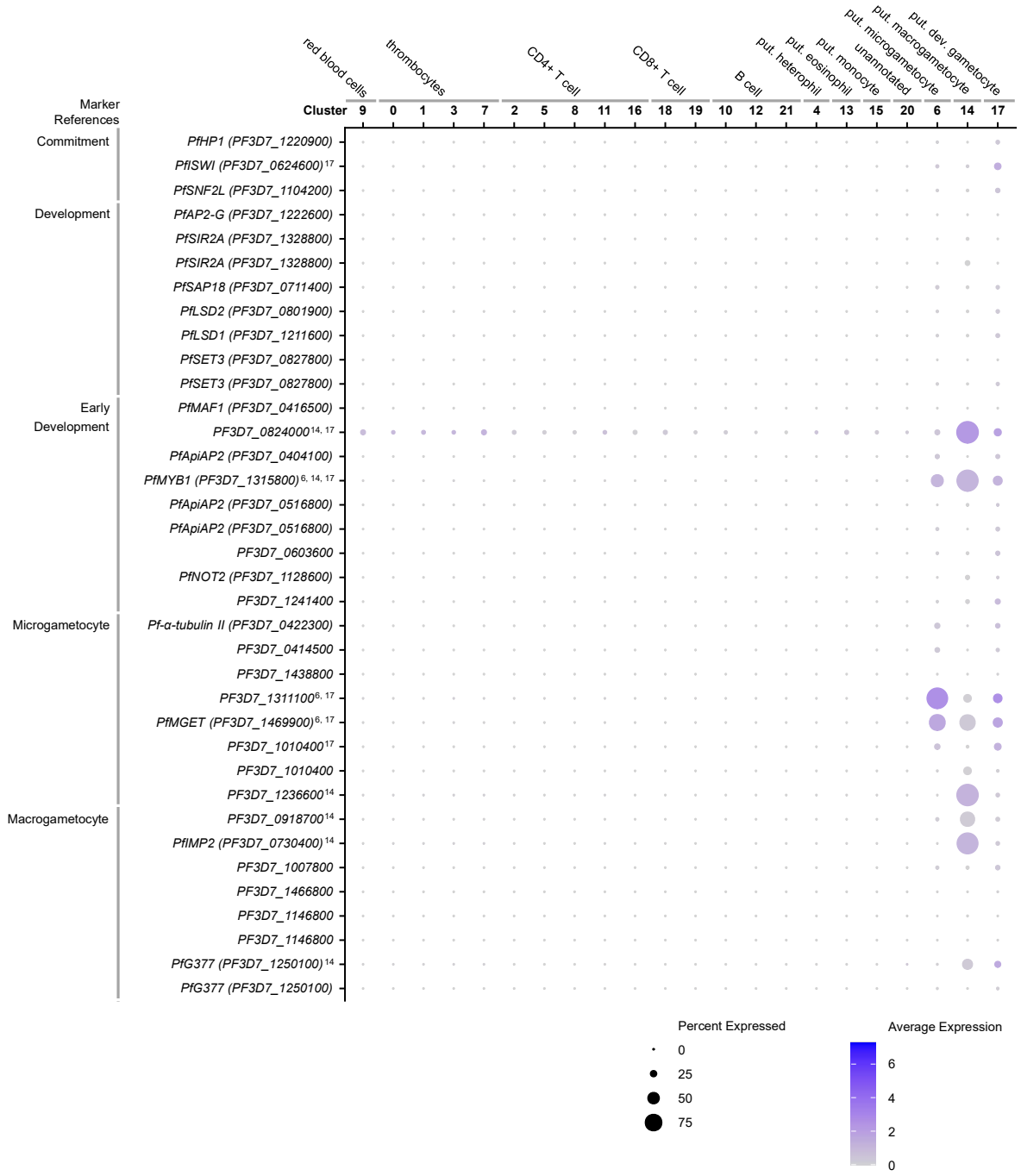

428

429 Figure S4: Dotplot of parasite marker genes from curated literature[75]. Clusters were ordered by
430 qualitative examination of marker gene expression under consideration of cluster distribution in Fig.
431 1A. Final annotations are indicated at the top of the plot. Annotations in superscript list clusters in
432 which a gene is differentially expressed in comparison to all clusters. Categories include commitment
433 to gametocytogenesis ("commitment") versus gametocytic development ("development"), early

434 gametocyte development and micro- and macrogametocyte specific markers. Duplicates are based on

435 two transcript variants mapped to the same gene.

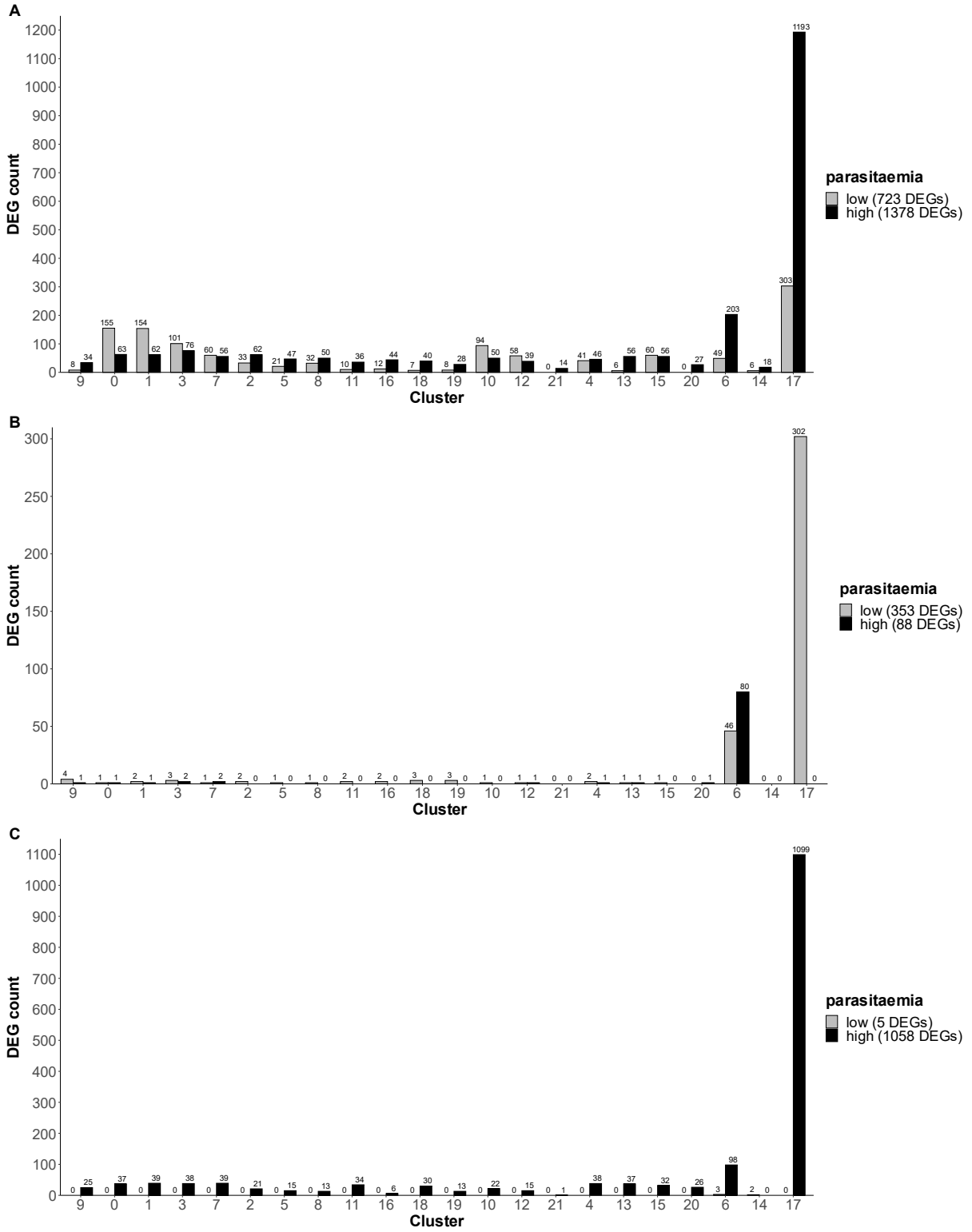

436

437 Figure S5: (A) Differentially expressed genes comparing LP versus HP per cluster (cut-off: p-value

438 (adjusted) ≤ 0.05). (B) Strongly differentially expressed host genes (cut-off: p-value (adjusted) ≤ 0.05;

439 $\log_2$-FC (averaged) ≥ 1) comparing LP versus HP per cluster. Unannotated genes were omitted (C):

440 Strongly differentially expressed parasite genes (cut-off: p-value (adjusted) ≤ 0.05; $\log_2$-FC (averaged)

441 ≥ 1) comparing LP versus HP per cluster. Unannotated genes were omitted. Clusters are ordered by

442 cell type.

443

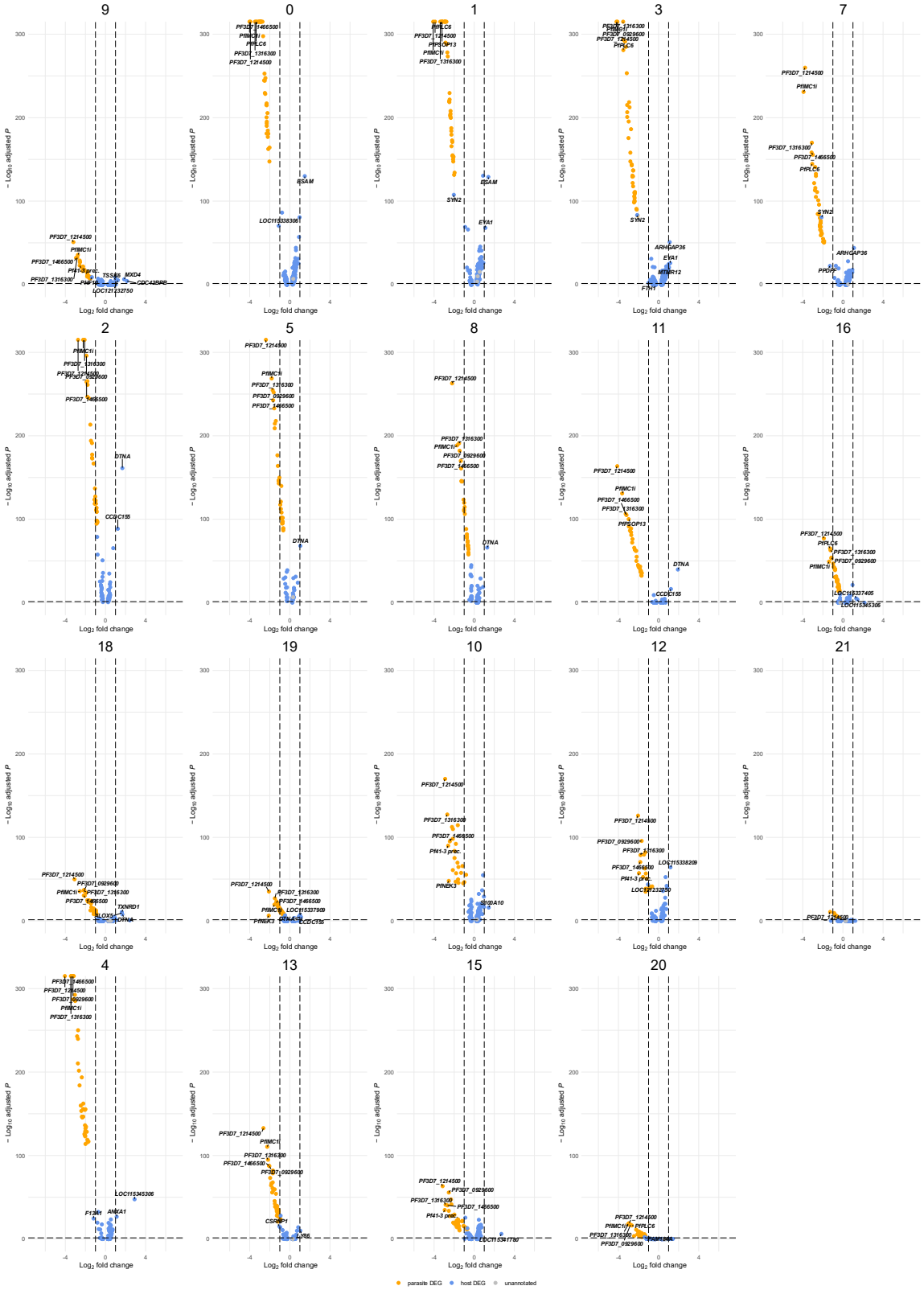

Figure S6: Differential gene expression across host clusters (top five host and parasite DEGs of LP versus HP are labelled). Dotted lines delimit cut-off-values (p-value (adjusted) ≤ 0.05; $\log_2$-FC (averaged) ≥ 1). Negative and positive values for $\log_2$-FC represent differential expression under HP versus LP respectively. Clusters are ordered by cell type.

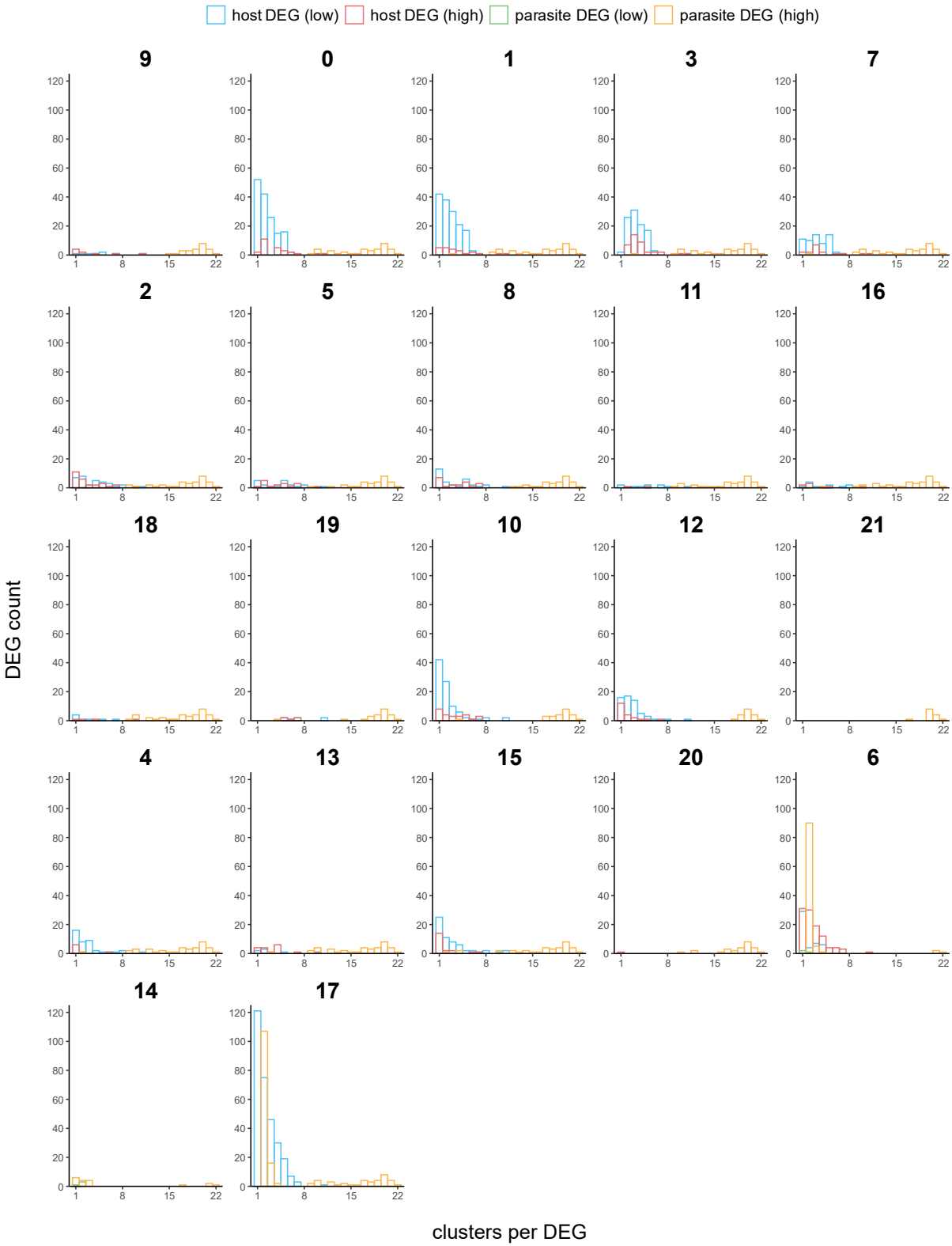

Figure S7: Redundancy of differentially expressed genes (cut-off: p-value (adjusted) ≤ 0.05). DEG counts are plotted against the number of clusters a gene is differentially expressed in. Unannotated genes were omitted.

453 ## References

454 1. Thompson JN. 1994. The coevolutionary process. Chicago. University of Chicago Press.

455 2. Windsor DA. 1998. Most of the species on Earth are parasites. International Journal for Parasitology.
456 28(12):1939–1941.

457 3. Schmid-Hempel P. 2009. Immune defence, parasite evasion strategies and their relevance for
458 'macroscopic phenomena' such as virulence. Philosophical Transactions of the Royal Society of London.
459 Series B, Biological Sciences. 364(1513):85–98.

460 4. Anderson RM, May RM. 1982. Coevolution of hosts and parasites. Parasitology. 85(2):411–426.

461 5. Ewald PW. 1983. Host-Parasite Relations, Vectors, and the Evolution of Disease Severity. Annual
462 Review of Ecology and Systematics. 14(1):465–485.

463 6. Day T. 2001. Parasite transmission modes and the evolution of virulence. Evolution. 55(12): 2389–
464 2400.

465 7. Day T. 2002. The evolution of virulence in vector-borne and directly transmitted parasites.
466 Theoretical Population Biology. 62(2):199–213.

467 8. Acevedo MA, Dillemuth FP, Flick AJ, Faldyn MZ, Elderd BD. 2019. Virulence-driven trade-offs in
468 disease transmission: A meta-analysis. Evolution. 73(4):636–647.

469 9. Ewald PW. 1987. Transmission modes and evolution of the parasitism-mutualism continuum. Annals
470 of the New York Academy of Sciences. 503:295–306.

471 10. Schmid-Hempel P. 2003. Variation in immune defence as a question of evolutionary ecology.
472 Proceedings of the Royal Society - Biological Sciences (Series B). 270(1513):357–366.

473 11. Deroost K, Pham T-T, Opdenakker G, van den Steen PE. 2016. The immunological balance between
474 host and parasite in malaria. FEMS Microbiology Reviews. 40(2):208–257.

475 12. Zambrano-Villa S, Rosales-Borjas D, Carrero JC, Ortiz-Ortiz L. 2002. How protozoan parasites evade
476 the immune response. Trends in Parasitology. 18(6):272–278.

477 13. Gomes PS, Bhardwaj J, Rivera-Correa J, Freire-De-Lima CG, Morrot A. 2016. Immune Escape
478 Strategies of Malaria Parasites. Frontiers in Microbiology. 7:1617.

479 14. Rénia L, Goh Y. S. 2016. Malaria Parasites: The Great Escape. Frontiers in Immunology. 7:463.

480 15. Cowman AF, Tonkin CJ, Tham W-H, Duraisingh MT. 2017. The Molecular Basis of Erythrocyte
481 Invasion by Malaria Parasites. Cell Host & Microbe. 22(2):232–245.

482 16. Rivero A, Gandon S. 2018. Evolutionary Ecology of Avian Malaria: Past to Present. Trends in
483 Parasitology. 34(8):712–726.

484 17. Pacheco MA, Matta NE, Valkiunas G, Parker PG, Mello B, Stanley Jr CE, Lentino M, Garcia-Amado
485 MA, Cranfield M, Kosakovsky Pond SL, Escalante AA. 2018. Mode and Rate of Evolution of
486 Haemosporidian Mitochondrial Genomes: Timing the Radiation of Avian Parasites. Molecular Biology
487 and Evolution. 35(2):383–403.

488 18. Valkiūnas G. 2005. Avian malaria parasites and other haemosporidia. Boca Raton: CRC Press.

489 19. Harl J, Himmel T, Valkiūnas G, Ilgūnas M, Nedorost N, Matt J, Kübber-Heiss A, Alic A, Konicek C,
490 Weissenböck H. 2022. Avian haemosporidian parasites of accipitriform raptors. Malaria Journal.
491 21(1):14.

492 20. Ottensmann M, Wiegmann A, Kruger O, et al. 2025. Surviving in a changing world: weather and
493 juvenile condition matter for a long-lived avian predator, but blood parasites do not appear to. Oikos
494 2025; 7.

495 21. Rinaud T, Ottensmann M, Rapp TM, et al. 2025. Blood parasite infection causes marginal
496 temporary costs in juvenile birds of prey. Front. Ecol. Evol.; 13.

497 22. Shutler D, Ankney CD, Mullie A. 1999. Effects of the blood parasite *Leucocytozoon simondi* on
498 growth rates of anatid ducklings. Canadian Journal of Zoology. 77(10):1573–1578.

499 23. Wiegmann A, Springer A, Rinaud T, Ottensmann M, Legler M, Krüger O, Fehr M, Chakarov N, Strube
500 C. 2021. The prevalence of *Leucocytozoon* spp. In nestlings of three wild raptor species including
501 implications on haematological and blood chemistry values. International Journal for Parasitology.
502 Parasites and Wildlife. 16:236–243.

503 24. Videvall E, Cornwallis CK, Palinauskas V, Valkiūnas G, Hellgren O. 2015. The avian transcriptome
504 response to malaria infection. Molecular Biology and Evolution. 32(5):1255–1267.

505 25. Outlaw DC, Walstrom VW, Bodden HN, Hsu C-Y, Arick 2nd M, Peterson DG. 2019. Molecular
506 evolution in immune genes across the avian tree of life. Parasitology Open. 5:e3363.

507 26. Videvall E, Palinauskas V, Valkiūnas G, Hellgren O. 2020. Host Transcriptional Responses to High-
508 and Low-Virulent Avian Malaria Parasites. The American Naturalist. 195(6):1070–1084.

509 27. Kalbskopf V, Ahrén D, Valkiūnas G, Palinauskas V, Hellgren O. 2021. Shifts in gene expression
510 variability in the blood-stage of *Plasmodium relictum*. Gene. 792:145723.

511 28. Dai M, Zhao L, Li Z, Li X, You B, Zhu S, Liao M. 2021. The Transcriptional Differences of Avian
512 CD4(+)CD8(+) Double-Positive T Cells and CD8(+) T Cells From Peripheral Blood of ALV-J Infected
513 Chickens Revealed by Smart-Seq2. Frontiers in Cellular and Infection Microbiology. 11:747094.

514 29. Liang Y, Ma Y, Zhang Y, Chen Z, Wang Z, Li X, Cui L, Xu L, Liu S, Li H. 2021. Single-Cell Analysis of the
515 In Vivo Dynamics of Host Circulating Immune Cells Highlights the Importance of Myeloid Cells in Avian
516 Flaviviral Infection. Journal of Immunology. 207(11):2878–2891.

517 30. Qu X, Li X, Li Z, Liao M, Dai M. 2022. Chicken Peripheral Blood Mononuclear Cells Response to Avian
518 Leukosis Virus Subgroup J Infection Assessed by Single-Cell RNA Sequencing. Frontiers in Microbiology.
519 13:800618.

520 31. Bean AG, Lowenthal JW. 2022. Avian cytokines and their receptors. Avian Immunology (Third
521 Edition). Cambridge, Massachusetts: Academic Press. 249–276.

522 32. Popa GL, Popa MI. 2021. Recent Advances in Understanding the Inflammatory Response in Malaria:
523 A Review of the Dual Role of Cytokines. Journal of Immunology Research. 2021:7785180.

524 33. Howick VM, Russell AJC, Andrews T, Heaton H, Reid AJ, Natarajan K, Butungi H, Metcalf T, Verzier
525 LH, Rayner JC, et al. 2019. The Malaria Cell Atlas: Single parasite transcriptomes across the complete
526 *Plasmodium* life cycle. Science. 365(6455):eaaw2619.

527 34. Brandler T, Chakarov N. 2024. Mitochondrial and apicoplast genome copy abundances of
528 haemosporidian parasites are explained by host species and parasitic lineage. Front. Ecol. Evol.
529 12:1305418.

530 35. Mair GR, Braks JAM, Garver LS, Wiegant JCAG, Hall N, Dirks RW, Khan SM, Dimopoulos G, Janse CJ,
531 Waters AP. 2006. Regulation of sexual development of *Plasmodium* by translational repression.
532 Science. 313(5787):667–669.

533 36. Zhao W, Liu J, Xu R, Zhang C, Pang Q, Chen X, Liu S, Hong L, Yuan J, Li X, et al. 2015. The Gametocytes
534 of *Leucocytozoon sabrazesi* Infect Chicken Thrombocytes, Not Other Blood Cells. PloS One.
535 10(7):e0133478.

536 37. Chagas CRF, Duc M, Gutiérrez-Liberato GA, et al. 2024. Host Cells of *Leucocytozoon* (Haemosporida,
537 Leucocytozoidae) Gametocytes, with Remarks on the Phylogenetic Importance of This Character.
538 Pathogens 2023; 12.

539 38. Groff TC, Lorenz TJ, Iezhova TA, et al. 2022. Description and molecular characterization of novel
540 *Leucocytozoon* parasite (Apicomplexa: Haemosporida: Leucocytozoidae), *Leucocytozoon polynuclearis*
541 n. sp. found in North American woodpeckers. Syst Parasitol; 99: 103–114.

542 39. Ferreira JL, Heincke D, Wichers JS, et al. 2020. The Dynamic Roles of the Inner Membrane Complex
543 in the Multiple Stages of the Malaria Parasite. Front Cell Infect Microbiol; 10: 611801.

544 40. McGovern KE and Wilson EH. 2013. Role of Chemokines and Trafficking of Immune Cells in Parasitic
545 Infections. Curr Immunol Rev; 9: 157–168.

546 41. Hakimi M-A and Bougdour A. 2015. *Toxoplasma*'s ways of manipulating the host transcriptome via
547 secreted effectors. Curr Opin Microbiol; 26: 24–31.

548 42. Mahanta A, Ganguli P, Barah P, et al. 2018. Integrative Approaches to Understand the Mastery in
549 Manipulation of Host Cytokine Networks by Protozoan Parasites with Emphasis on *Plasmodium* and
550 *Leishmania* Species. Front Immunol; 9: 296.

551 43. Takada H and Kurisaki A. 2015. Emerging roles of nucleolar and ribosomal proteins in cancer,
552 development, and aging. Cell Mol Life Sci; 72: 4015–4025.

553 44. Warncke JD and Beck H-P. 2019. Host Cytoskeleton Remodeling throughout the Blood Stages of
554 *Plasmodium falciparum*. Microbiol Mol Biol Rev; 83.

555 45. Villares M, Berthelet J and Weitzman JB. 2020. The clever strategies used by intracellular parasites
556 to hijack host gene expression. Semin Immunopathol; 42: 215–226.

557 46. Nájera CA, Batista MF, Meneghelli I, et al. 2021. Mixed signals - how *Trypanosoma cruzi* exploits
558 host-cell communication and signaling to establish infection. J Cell Sci; 134.

559 47. Matulova M, Rajova J, Vlasatikova L, et al. 2012. Characterization of chicken spleen transcriptome
560 after infection with *Salmonella enterica* serovar Enteritidis. PLoS One; 7: e48101.

561 48. Matulova M, Varmuzova K, Sisak F, et al. 2013. Chicken innate immune response to oral infection
562 with *Salmonella enterica* serovar Enteritidis. Vet Res; 44: 37.

563 49. Meitern R, Andreson R and Hõrak P. 2014. Profile of whole blood gene expression following
564 immune stimulation in a wild passerine. BMC Genomics; 15: 533.

565 50. Reiner NE, Ng W and McMaster WR. 1987. Parasite-accessory cell interactions in murine
566 leishmaniasis. II. *Leishmania donovani* suppresses macrophage expression of class I and class II major
567 histocompatibility complex gene products. J Immunol; 138: 1926–1932.

568 51. Reiner NE, Ng W, Ma T, et al. 1988. Kinetics of gamma interferon binding and induction of major
569 histocompatibility complex class II mRNA in *Leishmania*-infected macrophages. Proc Natl Acad Sci U S
570 A; 85: 4330–4334.

571 52. Lüder CG, Lang T, Beuerle B, et al. 1998. Down-regulation of MHC class II molecules and inability to
572 up-regulate class I molecules in murine macrophages after infection with *Toxoplasma gondii*. Clin Exp
573 Immunol; 112: 308–316.

574 53. Lüder CGK, Walter W, Beuerle B, et al. 2001. *Toxoplasma gondii* down-regulates MHC class II gene
575 expression and antigen presentation by murine macrophages via interference with nuclear
576 translocation of STAT1α. Eur. J. Immunol.; 31: 1475–1484.

577 54. Chakarov N, Pauli M and Krüger O. 2017. Immune responses link parasite genetic diversity,
578 prevalence and plumage morphs in common buzzards. Evol Ecol; 31: 51–62.

579 55. Nakamori M and Takahashi MP. 2011. The role of α-dystrobrevin in striated muscle. Int J Mol Sci;
580 12: 1660–1671.

581 56. Morimoto A, Shibuya H, Zhu X, et al. 2012. A conserved KASH domain protein associates with
582 telomeres, SUN1, and dynactin during mammalian meiosis. J Cell Biol; 198: 165–172.

583 57. Zhang J, Wang Y, Chu Y, et al. 2006. Agrin is involved in lymphocytes activation that is mediated by
584 alpha-dystroglycan. FASEB J; 20: 50–58.

585 58. González-Granado JM, Silvestre-Roig C, Rocha-Perugini V, et al. 2014. Nuclear envelope lamin-A
586 couples actin dynamics with immunological synapse architecture and T cell activation. Sci Signal; 7:
587 ra37.

588 59. Muri J, Heer S, Matsushita M, et al. 2018. The thioredoxin-1 system is essential for fueling DNA
589 synthesis during T-cell metabolic reprogramming and proliferation. Nat Commun; 9: 1851.

590 60. Lüder CGK, Algner M, Lang C, et al. 2003. Reduced expression of the inducible nitric oxide synthase
591 after infection with *Toxoplasma gondii* facilitates parasite replication in activated murine
592 macrophages. Int J Parasitol; 33: 833–844.

593 61. Calegari-Silva TC, Vivarini ÁC, Pereira RdMS, et al. 2018. *Leishmania amazonensis* downregulates
594 macrophage iNOS expression via Histone Deacetylase 1 (HDAC1): a novel parasite evasion mechanism.
595 Eur. J. Immunol.; 48: 1188–1198.

596 62. Brunet LR. 2001. Nitric oxide in parasitic infections. Int Immunopharmacol; 1: 1457–1467.

597 63. Ascenzi P, Bocedi A and Gradoni L. 2003. The anti-parasitic effects of nitric oxide. IUBMB Life; 55:
598 573–578.

599 64. Sobolewski P, Gramaglia I, Frangos J, et al. 2005. Nitric oxide bioavailability in malaria. Trends
600 Parasitol; 21: 415–422.

601 65. Gozzelino R, Andrade BB, Larsen R, et al. 2012. Metabolic adaptation to tissue iron overload confers
602 tolerance to malaria. Cell Host Microbe; 12: 693–704.

603 66. Ben-Othman R, Flannery AR, Miguel DC, et al. 2014. *Leishmania*-mediated inhibition of iron export
604 promotes parasite replication in macrophages. PLoS Pathog; 10: e1003901.

605 67. Ashford RW, Wyllie I and Newton I. 1990. *Leucocytozoon toddi* in British sparrowhawks *Accipiter*
606 *nisus* observations on the dynamics of infection. Journal of Natural History; 24: 1101–1107.

607 68. Chakarov N, Linke B, Boerner M, et al. 2015. Apparent vector-mediated parent-to-offspring
608 transmission in an avian malaria-like parasite. Mol Ecol; 24: 1355–1363.

609 69. Kaiser MI, Gadau J, Kaiser S, et al. 2024. Individualized social niches in animals: Theoretical
610 clarifications and processes of niche change. BioScience.

611 70. Butler A, Hoffman P, Smibert P, et al. 2018. Integrating single-cell transcriptomic data across
612 different conditions, technologies, and species. Nat Biotechnol; 36: 411–420.

613 71. Stuart T, Butler A, Hoffman P, et al. Comprehensive Integration of Single-Cell Data. Cell 2019; 177:
614 1888-1902.e21.

615 72. Hao Y, Hao S, Andersen-Nissen E, et al. Integrated analysis of multimodal single-cell data. Cell 2021;
616 184: 3573-3587.e29.

617 73. McGinnis CS, Murrow LM and Gartner ZJ. DoubletFinder: Doublet Detection in Single-Cell RNA
618 Sequencing Data Using Artificial Nearest Neighbors. Cell Syst 2019; 8: 329-337.e4.

619 74. van Biljon R, van Wyk R, Painter HJ, et al. Hierarchical transcriptional control regulates *Plasmodium*
620 *falciparum* sexual differentiation. BMC Genomics 2019; 20: 920.

621 75. Harmon BG. Avian heterophils in inflammation and disease resistance. Poult Sci 1998; 77: 972–977.

622 76. Swaggerty CL, Kogut MH, Ferro PJ, et al. Differential cytokine mRNA expression in heterophils
623 isolated from *Salmonella*-resistant and -susceptible chickens. Immunology 2004; 113: 139–148.

624 77. van Dijk A, Veldhuizen EJA and Haagsman HP. Avian defensins. Vet Immunol Immunopathol 2008;
625 124: 1–18.

626 78. Schmaier AA, Stalker TJ, Runge JJ, et al. Occlusive thrombi arise in mammals but not birds in
627 response to arterial injury: evolutionary insight into human cardiovascular disease. Blood 2011; 118:
628 3661–3669.

629 79. Scanes CG. Sturkie's Avian Physiology -Sixth Edition - Chapter 10 - Blood 2015: 167–191.

630 80. R Core Team. A language and environment for statistical computing 2021, https://www.R-
631 project.org/ (2021).

632 81. Shannon P, Markiel A, Ozier O, et al. Cytoscape: a software environment for integrated models of
633 biomolecular interaction networks 2003; Genome Research,: 2498–2504.

634 82. Szklarczyk D, Gable AL, Lyon D, et al. 2019. STRING v11: protein-protein association networks with
635 increased coverage, supporting functional discovery in genome-wide experimental datasets. Nucleic
636 Acids Res; 47: D607-D613.

637 83. Doncheva NT, Morris JH, Holze H, et al. 2022. Cytoscape stringApp 2.0: Analysis and Visualization
638 of Heterogeneous Biological Networks. J Proteome Res.

639 84. Lessard J, Wu JI, Ranish JA, et al. 2007. An essential switch in subunit composition of a chromatin
640 remodeling complex during neural development. Neuron; 55: 201–215.

641 85. Spiridonov NA, Wong L, Zerfas PM, et al. 2005. Identification and characterization of SSTK, a
642 serine/threonine protein kinase essential for male fertility. Mol Cell Biol; 25: 4250–4261.

643 86. Boros K, Lacaud G and Kouskoff V. 2011. The transcription factor Mxd4 controls the proliferation
644 of the first blood precursors at the onset of hematopoietic development in vitro. Exp Hematol; 39:
645 1090–1100.

646 87. Vasilevsky NA, Ruby CE, Hurlin PJ, et al. 2011. OX40 engagement stabilizes Mxd4 and Mnt protein
647 levels in antigen-stimulated T cells leading to an increase in cell survival. Eur J Immunol; 41: 1024–
648 1034.

649 88. Leung T, Chen XQ, Tan I, et al. 1998. Myotonic dystrophy kinase-related Cdc42-binding kinase acts
650 as a Cdc42 effector in promoting cytoskeletal reorganization. Mol Cell Biol; 18: 130–140.

651 89. Neefjes J, Jongsma MLM, Paul P, et al. 2011. Towards a systems understanding of MHC class I and
652 MHC class II antigen presentation. Nat Rev Immunol; 11: 823–836.

653 90. Nasdala I, Wolburg-Buchholz K, Wolburg H, et al. 2002. A transmembrane tight junction protein
654 selectively expressed on endothelial cells and platelets. J Biol Chem; 277: 16294–16303.

655 91. Wegmann F, Petri B, Khandoga AG, et al. ESAM supports neutrophil extravasation, activation of
656 Rho, and VEGF-induced vascular permeability. 2006. J Exp Med; 203: 1671–1677.

657 92. Greengard P, Valtorta F, Czernik AJ, et al. Synaptic vesicle phosphoproteins and regulation of
658 synaptic function. Science 1993; 259: 780–785.

659 93. Bhangu PS, Genever PG, Spencer GJ, et al. Evidence for targeted vesicular glutamate exocytosis in
660 osteoblasts. Bone 2001; 29: 16–23.

661 94. Maiole F, Tedeschi G, Candiani S, et al. Synapsins are expressed at neuronal and non-neuronal
662 locations in *Octopus vulgaris*. Sci Rep 2019; 9: 15430.

663 95. Cook PJ, Ju BG, Telese F, et al. Tyrosine dephosphorylation of H2AX modulates apoptosis and
664 survival decisions. Nature 2009; 458: 591–596.

665 96. Krishnan N, Jeong DG, Jung S-K, et al. Dephosphorylation of the C-terminal tyrosyl residue of the
666 DNA damage-related histone H2A.X is mediated by the protein phosphatase eyes absent. J Biol Chem
667 2009; 284: 16066–16070.

668 97. Hegde RS, Roychoudhury K and Pandey RN. The multi-functional eyes absent proteins. Crit Rev
669 Biochem Mol Biol 2020; 55: 372–385.

670 98. Nandurkar HH, Caldwell KK, Whisstock JC, et al. Characterization of an adapter subunit to a
671 phosphatidylinositol (3)P 3-phosphatase: identification of a myotubularin-related protein lacking
672 catalytic activity. Proc Natl Acad Sci U S A 2001; 98: 9499–9504.

673 99. Nandurkar HH, Layton M, Laporte J, et al. Identification of myotubularin as the lipid phosphatase
674 catalytic subunit associated with the 3-phosphatase adapter protein, 3-PAP. Proc Natl Acad Sci U S A
675 2003; 100: 8660–8665.

676 100. Hnia K, Vaccari I, Bolino A, et al. Myotubularin phosphoinositide phosphatases: cellular functions
677 and disease pathophysiology. Trends Mol Med 2012; 18: 317–327.

678 101. Fagerberg L, Hallström BM, Oksvold P, et al. Analysis of the human tissue-specific expression by
679 genome-wide integration of transcriptomics and antibody-based proteomics. Mol Cell Proteomics
680 2014; 13: 397–406.

681 102. Nam H, Jeon S, An H, et al. 2019. Critical roles of ARHGAP36 as a signal transduction mediator of
682 Shh pathway in lateral motor columnar specification. eLife 2019; 8.

683 103. Comer SP. 2021. Turning Platelets Off and On: Role of RhoGAPs and RhoGEFs in Platelet Activity.
684 Front Cardiovasc Med; 8: 820945.

685 104. Jiang Z, Song J, Qi F, et al. 2008. Exdpf is a key regulator of exocrine pancreas development
686 controlled by retinoic acid and ptf1a in zebrafish. PLoS Biol; 6: e293.

687 105. Yun M, Yingzi L, Jie G, et al. 2022. PPDPF Promotes the Progression and acts as an Antiapoptotic
688 Protein in Non-Small Cell Lung Cancer. Int J Biol Sci; 18: 214–228.

689 106. Tuohimaa P, Joensuu T, Isola J, et al. 1989. Development of progestin-specific response in the
690 chicken oviduct. Int J Dev Biol; 33: 125–134.

691 107. Loes AN, Bridgham JT and Harms MJ. 2018. Coevolution of the Toll-Like Receptor 4 Complex with
692 Calgranulins and Lipopolysaccharide. Front Immunol; 9: 304.

693 108. Cook-Moreau JM, El-Makhour Hojeij Y, Barrière G, et al. 2007. Expression of 5-lipoxygenase (5-
694 LOX) in T lymphocytes. Immunology; 122: 157–166.

695 109. Lone AM and Taskén K. 2013. Proinflammatory and immunoregulatory roles of eicosanoids in T
696 cells. Front Immunol; 4: 130.

697 110. Sun Q-Y, Zhou H-H and Mao X-Y. 2019. Emerging Roles of 5-Lipoxygenase Phosphorylation in
698 Inflammation and Cell Death. Oxidative Medicine and Cellular Longevity; 2019: 2749173.

699 111. Lanier LL. 2015. NKG2D Receptor and Its Ligands in Host Defense. Cancer Immunol Res; 3: 575–
700 582.

701 112. Lou Y, Han M, Liu H, et al. 2020. Essential roles of S100A10 in Toll-like receptor signaling and
702 immunity to infection. Cell Mol Immunol; 17: 1053–1062.

703 113. Francischetti IMB, Seydel KB and Monteiro RQ. 2008. Blood coagulation, inflammation, and
704 malaria. Microcirculation; 15: 81–107.

705 114. Sheikh MH and Solito E. 2018. Annexin A1: Uncovering the Many Talents of an Old Protein. Int J
706 Mol Sci; 19.

707 115. Pang J, Yu Q, Chen Y, et al. 2022. Integrating Single-cell RNA-seq to construct a Neutrophil
708 prognostic model for predicting immune responses in non-small cell lung cancer. J Transl Med; 20: 531.

709 116. Schultz TE and Blumenthal A. 2017. The RP105/MD-1 complex: molecular signaling mechanisms
710 and pathophysiological implications. J Leukoc Biol; 101: 183–192.

711 117. Sancho D and Reis e Sousa C. 2012. Signaling by myeloid C-type lectin receptors in immunity and
712 homeostasis. Annu Rev Immunol; 30: 491–529.

713 118. Liu L, Lin J and He H. 2019. Identification of Potential Crucial Genes Associated With the
714 Pathogenesis and Prognosis of Endometrial Cancer. Front Genet; 10: 373.

715 119. Huang W, Li G, Wang Z, et al. 2020. A Ten-N6-Methyladenosine (m6A)-Modified Gene Signature
716 Based on a Risk Score System Predicts Patient Prognosis in Rectum Adenocarcinoma. Front Oncol; 10:
717 567931.

718 120. Xing J, Shen S, Liu X, et al. 2022. A hypoxia-related prognostic model predicts overall survival and
719 treatment response in hepatocellular carcinoma. Biosci Rep; 42.

720 121. Meister A and Anderson ME. 1983. Glutathione. Annu Rev Biochem; 52: 711–760.

721 122. Brown GD, Willment JA and Whitehead L. 2018. C-type lectins in immunity and homeostasis. Nat
722 Rev Immunol; 18: 374–389.

723 123. Jonikas MC, Collins SR, Denic V, et al. 2009. Comprehensive characterization of genes required for
724 protein folding in the endoplasmic reticulum. Science; 323: 1693–1697.

725 124. Shurtleff MJ, Itzhak DN, Hussmann JA, et al. 2018. The ER membrane protein complex interacts
726 cotranslationally to enable biogenesis of multipass membrane proteins. eLife 2018; 7.

727 125. Verdot L, Lalmanach G, Vercruysse V, et al. 1996. Cystatins up-regulate nitric oxide release from
728 interferon-gamma-activated mouse peritoneal macrophages. J Biol Chem; 271: 28077–28081.

729 126. Das L, Datta N, Bandyopadhyay S, et al. 2001. Successful therapy of lethal murine visceral
730 leishmaniasis with cystatin involves up-regulation of nitric oxide and a favorable T cell response. J
731 Immunol; 166: 4020–4028.

732 127. Hartmann S, Schönemeyer A, Sonnenburg B, et al. 2002. Cystatins of filarial nematodes up-
733 regulate the nitric oxide production of interferon-gamma-activated murine macrophages. Parasite
734 immunology; 24: 253–262.

735 128. Johnson RD, Liu N and Jasin M. 1999. Mammalian XRCC2 promotes the repair of DNA double-
736 strand breaks by homologous recombination. Nature; 401: 397–399.

737 129. Deans B, Griffin CS, Maconochie M, et al. 2000. Xrcc2 is required for genetic stability, embryonic
738 neurogenesis and viability in mice. EMBO J; 19: 6675–6685.

739 130. Yuniati L, Scheijen B, van der Meer LT, et al. 2019. Tumor suppressors BTG1 and BTG2: Beyond
740 growth control. J Cell Physiol; 234: 5379–5389.

741 131. Damena D, Agamah FE, Kimathi PO, et al. 2021. Insilico Functional Analysis of Genome-Wide
742 Dataset From 17,000 Individuals Identifies Candidate Malaria Resistance Genes Enriched in Malaria
743 Pathogenic Pathways. Front Genet; 12: 676960.

744 132. Cohen S, Braiman A, Shubinsky G, et al. 2011. Protein kinase C-theta in platelet activation. FEBS
745 Lett; 585: 3208–3215.

746 133. Ivison SM, Graham NR, Bernales CQ, et al. 2007. Protein kinase D interaction with TLR5 is required
747 for inflammatory signaling in response to bacterial flagellin. J Immunol; 178: 5735–5743.

748 134. Zhang X, Connelly J, Chao Y, et al. 2021. Multifaceted Functions of Protein Kinase D in Pathological
749 Processes and Human Diseases. Biomolecules 2021; 11.

750 135. Bosco EE, Mulloy JC and Zheng Y. 2009. Rac1 GTPase: a "Rac" of all trades. Cell Mol Life Sci; 66:
751 370–374.

752 136. Xiong JW, Leahy A, Lee HH, et al. 1999. Vezf1: A Zn finger transcription factor restricted to
753 endothelial cells and their precursors. Dev Biol; 206: 123–141.

754 137. Niu J, Qin B, Wang C, et al. 2021. Identification of Key Immune-Related Genes in the Progression
755 of Septic Shock. Front Genet; 12: 668527.

756 138. Ravel DB. 2017. Mechanisms of Cellular Remodeling during *Plasmodium falciparum* Sequestration
757 and Transmission; Doctoral dissertation, Harvard University, Graduate School of,
758 http://nrs.harvard.edu/urn-3:HUL.InstRepos:42061497 (2017, accessed 19 January 2023).

759 139. Vaid A and Sharma P. 2006. PfPKB, a protein kinase B-like enzyme from *Plasmodium falciparum*:
760 II. Identification of calcium/calmodulin as its upstream activator and dissection of a novel signaling
761 pathway. J Biol Chem; 281: 27126–27133.

762 140. Vaid A, Thomas DC and Sharma P. 2008. Role of Ca2+/calmodulin-PfPKB signaling pathway in
763 erythrocyte invasion by Plasmodium falciparum. J Biol Chem; 283: 5589–5597.

764 141. Ecker A, Bushell ESC, Tewari R, et al. 2008. Reverse genetics screen identifies six proteins
765 important for malaria development in the mosquito. Mol Microbiol; 70: 209–220.

766 142. Lye YM, Chan M and Sim T-S. 2006. Pfnek3: an atypical activator of a MAP kinase *in Plasmodium*
767 *falciparum*. FEBS Lett; 580: 6083–6092.

768 143. Capelli-Peixoto J, Saelao P, Johnson WC, et al. 2022. Comparison of high throughput RNA
769 sequences between *Babesia bigemina* and *Babesia bovis* revealed consistent differential gene
770 expression that is required for the Babesia life cycle in the vertebrate and invertebrate hosts. Front
771 Cell Infect Microbiol; 12: 1093338.

772 144. Boucher MJ, Ghosh S, Zhang L, et al. 2018. Integrative proteomics and bioinformatic prediction
773 enable a high-confidence apicoplast proteome in malaria parasites. PLoS Biol; 16: e2005895.

774 145. Wong W, Bai X, Brown A, et al. 2014. Cryo-EM structure of the *Plasmodium falciparum* 80S
775 ribosome bound to the anti-protozoan drug emetine. eLife 2014; 3.

776 146. Bzik DJ, Fox BA and Gonyer K. 1993. Expression of *Plasmodium falciparum* lactate dehydrogenase
777 in *Escherichia coli*. Mol Biochem Parasitol; 59: 155–166.

778 147. Makler MT and Hinrichs DJ. 1993. Measurement of the lactate dehydrogenase activity of
779 *Plasmodium falciparum* as an assessment of parasitemia. Am J Trop Med Hyg; 48: 205–210.

780 148. Mony BM, Mehta M, Jarori GK, et al. 2009. Plant-like phosphofructokinase from *Plasmodium*
781 *falciparum* belongs to a novel class of ATP-dependent enzymes. Int J Parasitol; 39: 1441–1453.

782 149. Rahlfs S, Fischer M and Becker K. 2001. *Plasmodium falciparum* possesses a classical glutaredoxin
783 and a second, glutaredoxin-like protein with a PICOT homology domain. J Biol Chem; 276: 37133–
784 37140.

785 150. Tajedin L, Anwar M, Gupta D, et al. 2015. Comparative insight into nucleotide excision repair
786 components of *Plasmodium falciparum*. DNA Repair (Amst); 28: 60–72.

787 151. Chung D-WD, Ponts N, Prudhomme J, et al. 2012. Characterization of the ubiquitylating
788 components of the human malaria parasite's protein degradation pathway. PLoS One; 7: e43477.

789 152. Goyal M, Heinberg A, Mitesser V, et al. 2021. Phosphorylation of the Canonical Histone H2A Marks
790 Foci of Damaged DNA in Malaria Parasites. mSphere 2021; 6.

791 153. Guttery DS, Poulin B, Ramaprasad A, et al. 2014. Genome-wide functional analysis of *Plasmodium*
792 protein phosphatases reveals key regulators of parasite development and differentiation. Cell Host
793 Microbe; 16: 128–140.